FILE COPY

Research Report

EVERGREEN POINT BRIDGE
MAINTENANCE PROBLEMS

ANNUAL REPORT

AUGUST 1978

Public Transportation and Planning Division

Washington State
Department of Transportation

In cooperation with
U.S. Department of Transportation
Federal Highway Administration

WA-RD-44.5

TECHNICAL REPORT STANDARD TITLE PAGE

1. Report No.	2. Government Accession No.	3. Recipient's Catalog No.
WA-RD-44.5		

4. Title and Subtitle	5. Report Date
Evergreen Point Bridge Maintenance Problems	August 1978
	6. Performing Organization Code
7. Author(s)	8. Performing Organization Report No.
C. B. Brown	
9. Performing Organization Name and Address	10. Work Unit No.
University of Washington Seattle, Washington 98195	Y-1640
	11. Contract or Grant No.
	13. Type of Report and Period Covered
12. Sponsoring Agency Name and Address	Annual 1978
Washington State Department of Transportation Highway Administration Building Olympia, Washington 98504	14. Sponsoring Agency Code

15. Supplementary Notes

This study was conducted in cooperation with the U.S. Department of Transportation, Federal Highway Administration

16. Abstract

This report includes a full year of field data and a synthesis of all data. These include 422 hourly events of which 351 occurred in the 1977-78 season. The use of Miner's hypothesis is justified in this report.

17. Key Words	18. Distribution Statement
bridge, fatigue, reliability, wind	None

19. Security Classif. (of this report)	20. Security Classif. (of this page)	21. No. of Pages	22. Price
Unclassified	Unclassified	64	

Form DOT F 1700.7 (8-69)
HWY FORM 341-004 6/72

EVERGREEN POINT BRIDGE MAINTENANCE PROBLEMS

Principal Investigator

C. B. Brown

Department of Civil Engineering
University of Washington

(Fourth Annual Report)

Research Project Y-1640
Phase IV

Prepared for
Washington State Transportation Commission
Department of Transportation
in cooperation with
U.S. Department of Transportation
Federal Highway Administration

August 1978

APPENDIX

Values of parameters used to obtain life prediction in Tables 1 to 4.

Table 1:

Henry

$S_E = 39$ ksi

Manson

$N_R = 1000$ cycles

Valluri

$S_{E,1} = S_{E,2} = 39$ ksi

$S_i = -S_{i,min}$

Table 2:

Henry

$S_E = 85$ ksi

Generalized Henry

$b = 9.2$

Manson

$N_R = 1000$ cycles

Valluri

$S_{E,1} = S_{E,2} = 85$ ksi

The contents of this report reflects the views of the author who is responsible for the facts and the accuracy of the data presented herein. The contents do not necessarily reflect the official views or policies of the Washington State Department of Highways or the Federal Highway Administration. This report does not constitute a standard, specification, or regulation.

INTRODUCTION

This year's work (1977-78) has had the following phases:

1) maintenance of instrumentation and collection of field data
2) design of the laboratory fatigue testing appartus and the performance of fatigue tests on six trunnion anchorage rods
3) the comparison of fatigue theories to determine the validity of Miner's approach, which is the backbone of this study
4) analytical work which utilizes the parts (1) and (2) above to make statements concerning the maintenance of the drawspan elements.

A full year of data from field measurements was obtained. Appendix A displays the reduced data for the year. This work was in the hands of Mr. Donald Christensen, Research Engineer. The design, construction and operation of the laboratory fatigue endeavour was in the hands of Mr. Michael Landy, Research Assistant. Another Research Assistant, Mr. Ade Bright, investigated the validity of Miner's hypothesis. Mr. Christensen was involved in the analytical work. The project was under the direct supervision of the Principal Investigator.

This report includes extracts from the M.S.E. thesis of Mr. Landy to describe part (2) and the M.S.C.E. thesis of Mr. Bright to describe part (3). The original page numbering has been retained.

A final report of the whole project has been prepared and transmitted separately. It is intended to transmit this for possible publication under the authorship of Brown, Christensen, Landy and Vasu.

INSTRUMENTATION AND DATA

The instrumentation remained essentially unchanged from the previous year of work. The gauges on the anchorage cables were abandoned because they were continually being disturbed during normal bridge maintenance. The upkeep of the instrumentation and recording devices was a continual task over this season. The data were abundant which resulted in considerable time being necessary in collection and replacement of parts.

This year 351 hourly events over 20 mph were recorded. This compares with the 71 hourly events recorded in previous seasons. The data are presented in reduced form in Appendix A.

LABORATORY FATIGUE TESTS

A full description of these is given in the M.S.E. thesis of Mr. Mwchael Allen Landy. This thesis follows in its original form.

University of Washington

ABSTRACT

DEVELOPMENT OF A TEST PROGRAM TO OBTAIN S-N DATA FOR EVERGREEN POINT FLOATING BRIDGE VERTICAL TRUNNION ANCHORAGE RODS

By Michael Allen Landy

Chairperson of the
Supervisory Committee: Professor Colin B. Brown,
Department of Civil Engineering

Development of a test program to obtain empirical S-N data to be used in cumulative damage fatigue analyses is reported. The member under investigation is a vertical trunnion anchorage rod, a component of the drawspan section, Evergreen Point Floating Bridge, Lake Washington, Seattle, Washington. The Prot method of accelerated testing to obtain the fatigue limit and an extension of the Prot theory by Basavaraju and Lim were utilized to determine the S-N curve. Areas discussed included specimen description, fixture design, determination of magnitude and pattern of loading, instrumentation, and test results.

TABLE OF CONTENTS

LIST OF FIGURES

LIST OF TABLES

ACKNOWLEDGMENTS

The author would like to express his gratitude to Prof. Colin B. Brown for his guidance and assistance during the author's term as a Research Assistant. The author would also like to thank Prof. N. M. Hawkins, Prof. C. W. Roeder, Mr. D. R. Christenson, and Mr. T. McKay for assistance in fixture design and test setup; the staff of the Structures Laboratory under Mr. Ralph Bergman for fixture assembly and test support, and Ms. Carolynn Padgett for typing this report.

This work was funded by the Washington State Highway Department.

Section I: Introduction

Serious maintenance problems have prevented normal operation of the drawspan section of the Evergreen Point Floating Bridge over Lake Washington, Seattle, Washington. These problems are caused by fatigue failure of a number of drawspan components. Several investigations have been undertaken as part of a continuing study of these problems (1,2,3). These investigations dealt with mehtods of fatigue analysis and the application of these analyses to drawspan components. These investigations made use of one or more of the cumulative damage theories of fatigue, such as the well-known Palmgren-Miner hypothesis (4,5). These theories have been the subject of extensive research and exhaustive literature is available (6,7,8 and many others).

Common to all of the cumulative damage theories is the use of the S-N curve (Fig. 1). This curve is a plot of stress (S) versus number of cycles to failure (N). At the time of the earlier investigations of the Evergreen Point Bridge problems, empirical S-N curves were not available.

The purpose of this paper is to describe a test program designed to derive an S-N curve for one of the drawspan components, a vertical trunnion anchorage rod, where a record of service failures exists. This test program was designed subject to certain constraints. They were:

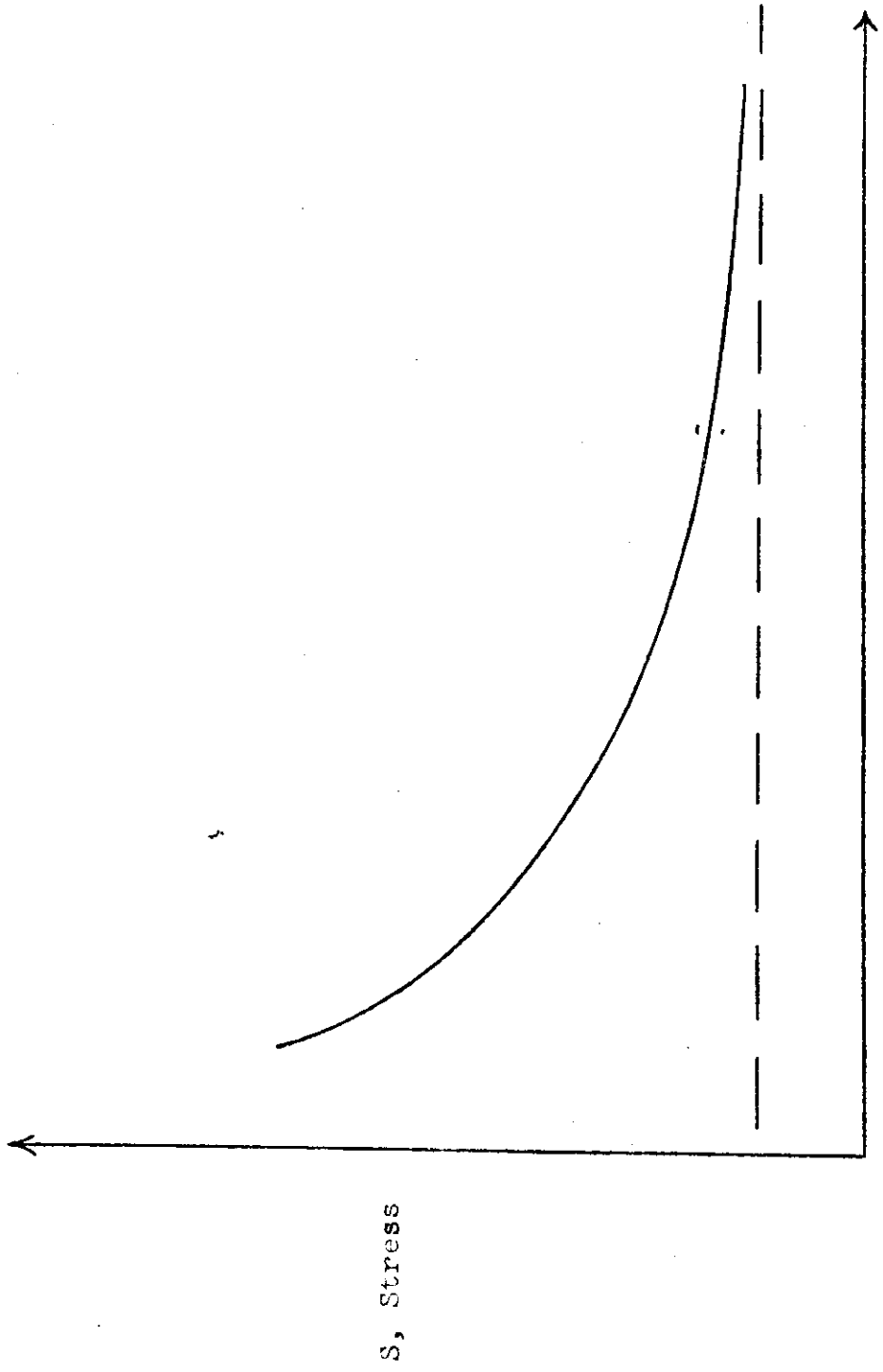

Fig. 1 THE S-N CURVE

1) Use existing concrete test pad in the University of Washington Civil Engineering Structural Test Laboratory (tie-downs subject to loading constraints),

2) Use available materials in the Structures Laboratory stockpile for the test fixture,

3) Use a 55 kip Materials Testing System Corp. (MTS Corp.) hydraulic load actuator and available electronic controllers to form a closed-loop electro-hydraulic fatigue machine capable of producing the desired magnitude and pattern of loading, and,

4) Obtain a useful S-N curve with six specimens, each being an actual rod taken from service prior to failure.

Historically, many investigators have found that six specimens do not constitute a large enough sample to determine a realistic S-N curve, due to the excessive amounts of "scatter" in the experimental data. This effect is even more pronounced when testing for the fatigue limit. For this reason, an alternative approach to normal constant amplitude cyclic testing at a single value of maximum and minimum stress was thought necessary. The Prot method (9) of accelerated testing to obtain the fatigue limit and Basavaraju and Lim's extension to the theory (10) to obtain an S-N curve from the Prot data was found to be appropriate.

This report will discuss a number of different areas of test program design. Among these shall be included specimen description, fixture design, determination of magnitude and pattern of loading, instrumentation, and test results.

Section II: Vertical Trunnion Anchorage Rod

2.1 Component Description

The vertical trunnion anchorage rod is made from a three-inch diameter AISI 4140 steel rod. The rods are 14 feet - 3 3/4 inches to 16 feet - 7 inches in length with six inches of 3-4 UNC-2A thread at both ends (Fig. 2a). Chemical and material properties tests on a typical rod show that the specimen tested meets ASTM A193-B7, the specification for this material. Results are shown in Table 1 (11). Although a Rockwell hardness test was not performed at that time, a reasonable estimate was obtained using a properties chart for AISI 4140 (12). Such data shows a Rockwell hardness value of C30 to be typical of AISI 4140 in this condition. After testing the Rockwell hardness was measured and found to be C26.

These rods have been failing in service due to crack initiation and propagation at the root of a thread, caused by cyclic tensile loading (Fig. 2b). This loading pattern is caused by the action of wind-generated water waves impinging on the side of the bridge (1,3). There are 12 such rods in the drawspan section.

2.2 Test Specimen

Six rods were taken from service to be used, as delivered, as full-size test specimens. The length of time in service is unknown and they have been stored unprotected in the atmosphere for about one year, prior to testing

a. Vertical trunnion anchorage rod

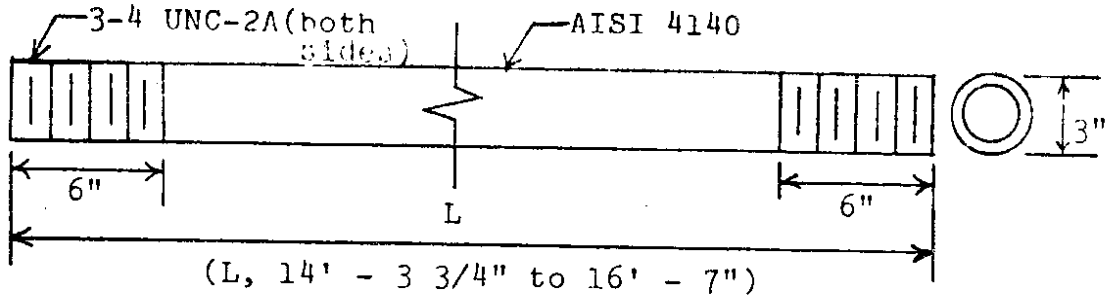

b. Failure location

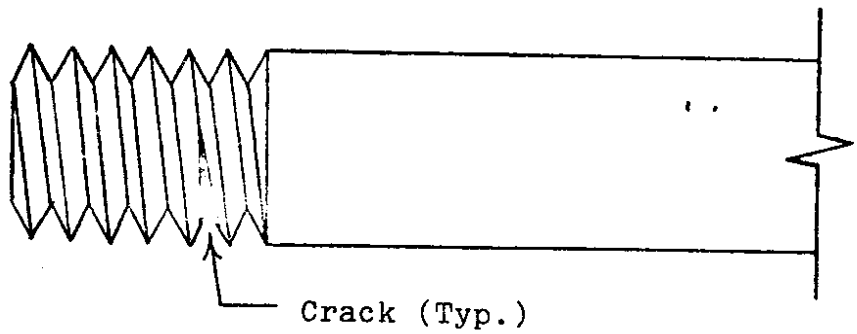

c. Test specimens

Fig. 2 VERTICAL TRUNNION ANCHORAGE ROD

Chemical composition

C	Mn	P	S	Si	Ni	Cr	Mo	V
.42	.93	.018	.025	.26	--	.98	.19	-

Material properties

Tensile strength (psi)	137,400
Yield strength (psi)	111,740
Elongation (percent in 2")	19.5
Percent reduction in area	58.4
BHN hardness	280
Minimum tempering temperature (°F)	1100
Modulus of elasticity (psi)	31.25×10^6

TABLE 1 CHEMICAL AND MATERIAL PROPERTIES, VERTICAL TRUNNION ANCHORAGE ROD.

(Fig. 2c). They were not moved during that time. Surface corrosion was evident, as shown in Figs. 3a-c.

Fig. 3 SURFACE CONDITIONS OF TEST SPECIMENS

Section III: Test Program

3.1 Determination of the S-N Curve

A normal test program for an S-N curve consists of applying stress cycles of a constant magnitude until failure occurs. Fig. 4 depicts a stress cycle and relevant parameters,

S_{max} = maximum value of applied stress in the cycle,

S_{min} = minimum value of applied stress in the cycle,

S_{mean} = mean stress = $(S_{max} + S_{min})/2$,

S_r = stress range = $S_{max} - S_{min}$,

S_a = stress amplitude = $S_r/2$,

R = stress ratio = S_{min}/S_{max} , and

A = stress ratio = S_a/S_{mean}.

The failure determines a point on the S-N curve. By testing a number of specimens at different magnitudes, the curve is determined.

The ordinate (stress) on the S-N curve (Fig. 1) may be S_{max}, S_{min}, or S_a. S_{max} or S_{min}, in combination with a specified value of R, or S_a, in combination with a specified value of A determines the magnitude of the stress cycle. Typically, S-N curves are generated with fully reversed loading, i.e., R = -1, and S_{max} as the ordinate. The value of stress below which failure will

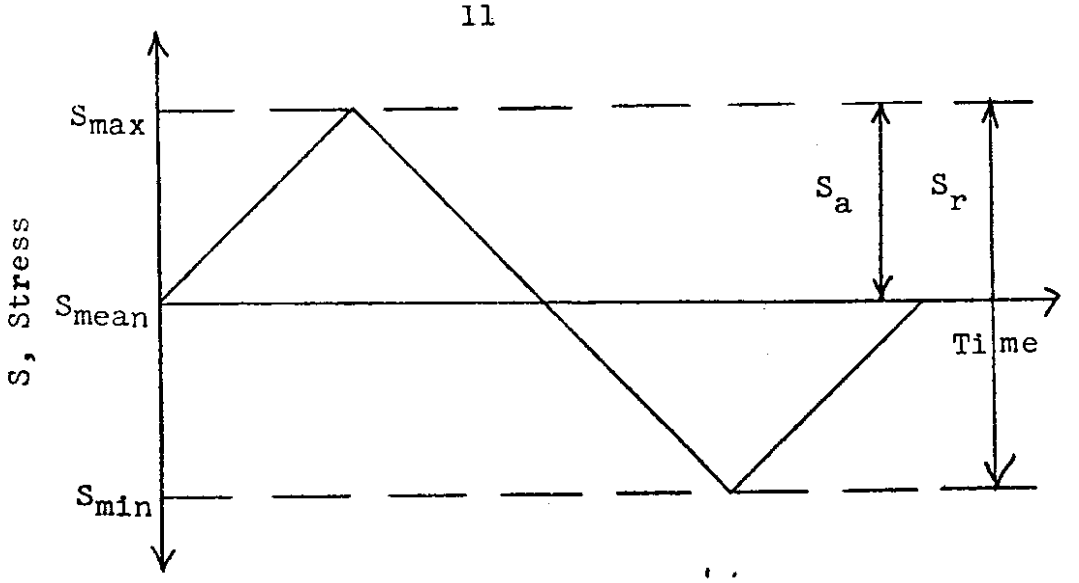

S_{max} = maximum value of applied stress in the cycle.

S_{min} = minimum value of applied stress in the cycle.

S_{mean} = mean stress in the cycle = $(S_{max} + S_{min})/2$.

S_r = stress range = $S_{max} - S_{min}$.

S_a = stress amplitude = $S_r/2$.

R = stress ratio = S_{min}/S_{max}.

A = stress ratio = S_a/S_{mean}.

Fig. 4 THE STRESS CYCLE

not occur, regardless of the number of applied cycles, is the fatigue limit, S_f (Fig. 1).

3.2. Determination of the Magnitude of Stresses

Lee and Uhlig carried out fatigue tests (R = -1) on AISI 4140 steel specimens of various heat treatments while investigating corrosion fatigue (13). During this investigation, specimens were tested that had chemical and material properties similar to those of the anchorage rods. The properties are compared in Table 2. The S-N curve obtained by Lee and Uhlig, in dry air and 93% relative humidity, is shown in Fig. 5. Note that the minimum fatigue limit was found to be on the order of 65,000 psi. Other data available (14) shows similar values (on the order of 70,000 psi, minimum) for fully reversed test specimens. Cycling at R = 0 and similar values of S_{max} (i.e., anchorage rod conditions) would result in a greater fatigue life at any S_{max} and a higher fatigue limit, based on normal behavior of engineering materials.

Strain gauge measurements on in-place anchorage rods show a maximum net section stress level of approximately 30,000 psi. This is far below the fatigue limit suggested by any available data. Thus, it is apparent that failure must be occurring where a stress concentration has raised the local stress level to a point that would cause failure. Such stress concentrations exist at the roots of the threads and, in fact, this area is the site

Chemical properties

	C	Mn	P	S	S	N_a	Ca	Mo	V	N	Al
Anchorage rod	.42	.93	.018	.025	.26	-	.98	.19	-	N/R	N/R
Lee & Uhlig	.41	.81	.012	.015	.27	.1	.99	.16	N/R	.013	.044

Material properties	Anchorage rod	Lee & Uhlig
Tensile strength (psi)	137,400	141,000
Yield strength (psi)	117,740	125,000
Rockwell C hardness	30 (est.)	28 ± 1

TABLE 2. COMPARISON OF CHEMICAL AND MATERIAL PROPERTIES

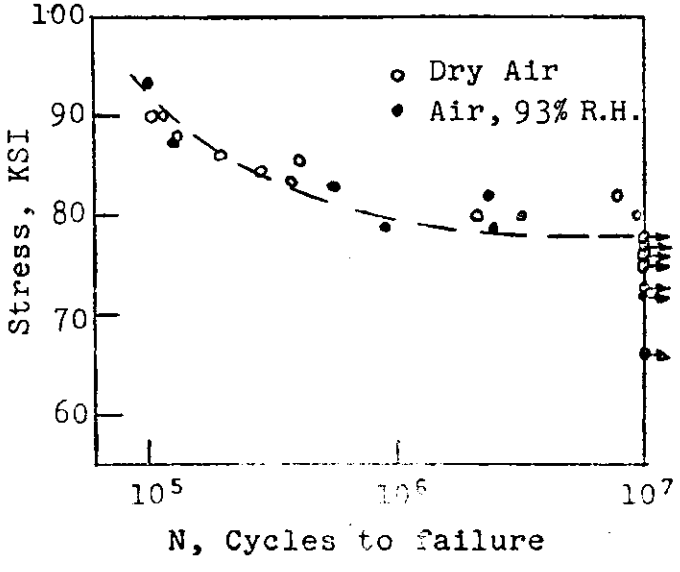

Fig. 5. S-N CURVE FOR 4130 STEEL, LEE & UHLIG (14)

of service failures.

The stress concentration factor, K_t, is defined as the ratio of the local stress in the vicinity of a notch or other stress concentrator to the net section stress (15). For the anchorage rod thread geometry,

$$K_t = 5.7$$

using the methods of Peterson (16) as described by Osgood (7, see Appendix A). The fatigue notch factor, K_f, is defined as the ratio of the fatigue strength of a specimen with no stress concentration to the fatigue strength at the same number of cycles with stress concentration, for the same conditions. For this particular case,

$$K_f = 4.8 \text{ (Appendix A)}.$$

Theoretically, by dividing the ordinate of an S-N curve by K_f, an S-N curve for the stress concentration is obtained.

By dividing the ordinate of Lee and Uhlig's curve (Fig. 5) by 4.8, the fatigue limit for R = -1 is reduced to approximately 13,500 psi. Although it cannot be stated how much higher this limit would be for anchorage rod conditions (R = 0), the possibility of a fatigue limit less than 30,000 psi is evident. The preceeding results suggested that the test specimens need not be taken to a net section stress level greater than 31,000 psi, the maximum <u>in situ</u> measured value. The fatigue

fixture was designed to take the specimens to 39,000 psi to provide a 25% margin for error.

3.3 Determination of the Loading Pattern

Generally, a different S-N curve must be generated for each specimen type, material condition, shape, test parameter (i.e., R), etc. A large number of curves are required to completely characterize the fatigue behavior of a material. Additionally, "scatter" is an inherent characteristic of fatigue test results and a large number of specimens are usually required to define a single S-N curve. The number of specimens necessary to define just the fatigue limit can be large and the tests lengthy. As only six specimens were available to determine the S-N curve and the fatigue limit, an alternative approach to constant amplitude testing was thought necessary.

The Prot method (9) of accelerated fatigue testing to determine the fatigue limit was found to be appropriate. Prot reported that it was possible to obtain a good approximation of the fatigue limit with five or six specimens. The method involves cycling the specimen with a loading pattern in which the stress amplitude increases linearly with respect to cycle. The pattern is depicted for R = -1 and R = 0 in Fig. 6. The accelerated fatigue test failure stress is S_d, the cycles to failure are N_f, and the rate of increase is $\dot{S}$ (stress/cycle). Prot plotted S_d versus $\dot{S}^{\frac{1}{2}}$ for a number of different $\dot{S}$ and found

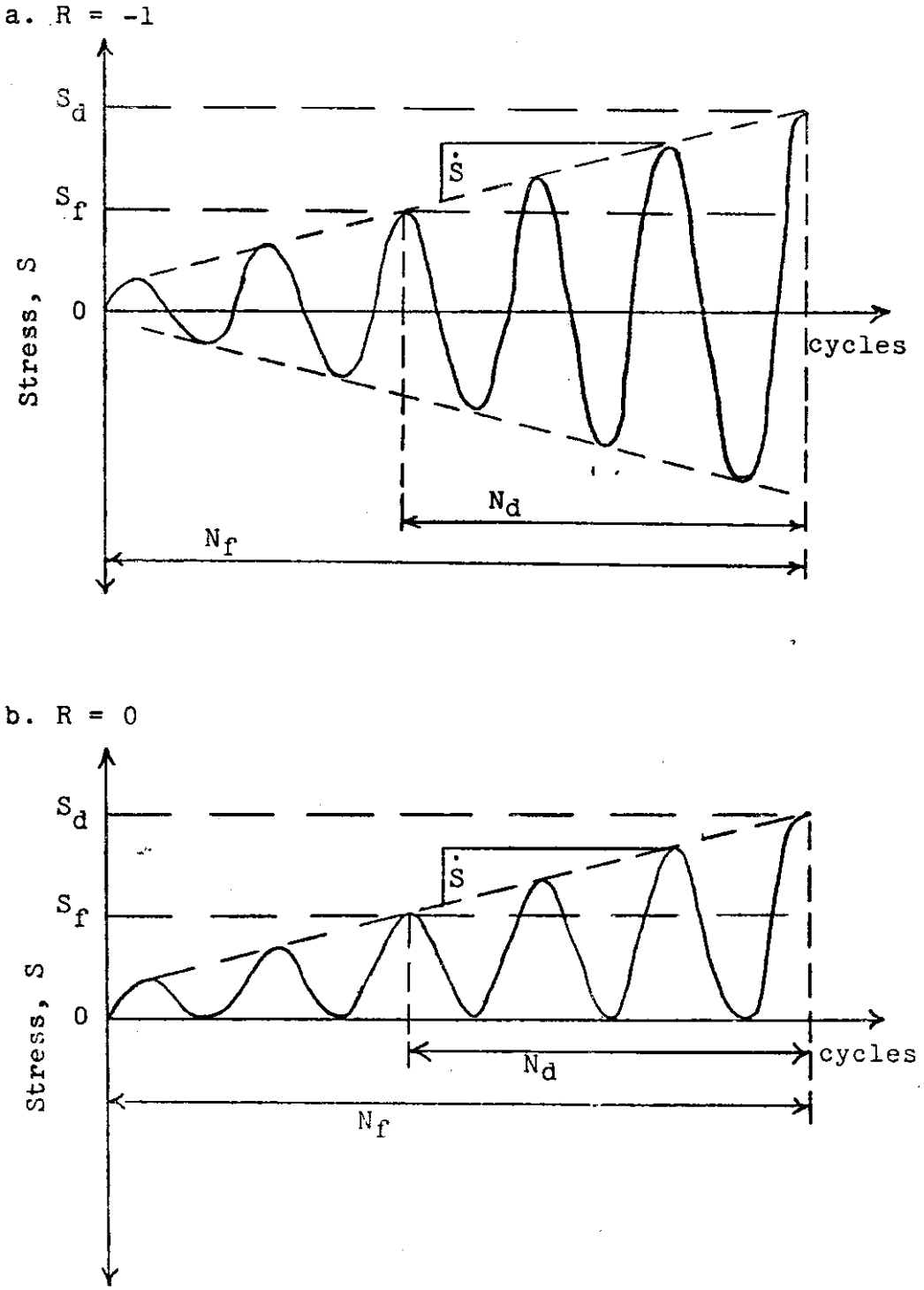

Fig. 6 LOADING PATTERNS FOR PROT TEST

that the data could be represented by a straight line that intersected the ordinate (S_d) at the fatigue limit (Fig. 7a).

Analytically, the result is obtained by assuming 1) that cycles accumulated below the fatigue limit do not cause structural damage and therefore the number of cycles causing structural damage, N_d, is (Fig. 6)

$$N_d = (S_d - S_f)/\dot{S} \ , \qquad 4.1$$

and 2) that the conventional S-N curve and accelerated fatigue $S_d - N_d$ curve are hyperbolas asymptotic to the fatigue limit and the vertical axis (Fig. 7b):

$$(S - S_f)\, N = C \ , \qquad 4.2$$

and

$$(S_d - S_f)\, N_d = C_d \ , \qquad 4.3$$

respectively, where

C, C_d = constants.

Recalling that

$$N_d = (S_d - S_f)/\dot{S} \ , \qquad 4.1$$

N_d can be eliminated from 4.3 by substituting 4.1:

$$(S_d - S_f)(S_d - S_f)/\dot{S} = C_d$$

$$(S_d - S_f)^2 = C_d \dot{S}$$

$$S_d - S_f = C_d^{\frac{1}{2}} \dot{S}^{\frac{1}{2}}$$

$$S_d = S_f + C_d^{\frac{1}{2}} \dot{S}^{\frac{1}{2}} \ . \qquad 4.4a$$

a. Prot equation

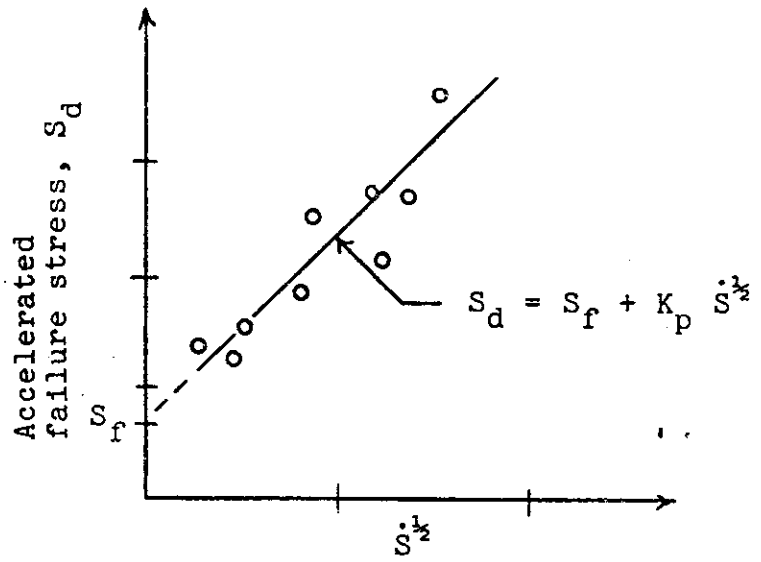

b. Hyperbolic shape assumptions

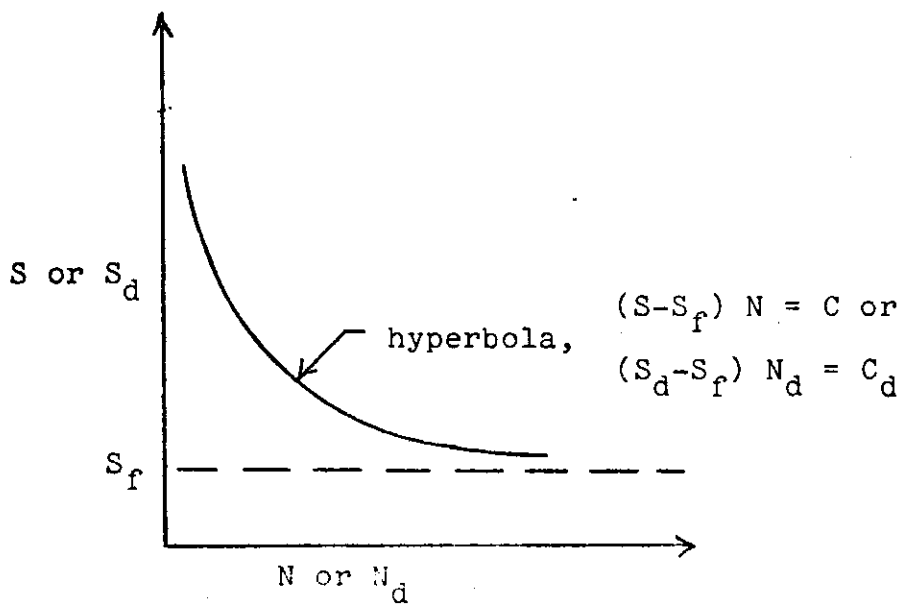

Fig. 7 ACCELERATED FATIGUE MODEL

Let

$$C_d^{\frac{1}{2}} = \text{constant} = K_p \qquad 4.4b$$

and, thus

$$S_d = S_f + K_p \dot{S}^{\frac{1}{2}} \qquad 4.4c$$

which is the equation of the line in Fig. 7a.

Subsequent investigations (17,18) have modified the Prot assumptions by using higher order hyperbolas:

$$(S - S_f)^m N = C \qquad 4.5$$

and

$$(S_d - S_f)^r N_d = C_d \qquad 4.6$$

Following the same mathematical procedure as in the preceding derivation, 4.6 becomes

$$S_d = S_f + C_d^{\frac{1}{r+1}} \dot{S}^{\frac{1}{r+1}} \qquad 4.7a$$

Let

$$\frac{1}{r+1} = \text{constant} = k \qquad 4.7b$$

and

$$C_d^{\frac{1}{r+1}} = C_d^k = \text{constant} = K \qquad 4.7c$$

and, thus

$$S_d = S_f + K \dot{S}^k \ . \qquad 4.7d$$

This generalized form of the Prot equation removes the constraint that the power to which $\dot{S}$ is raised be equal to one half. By using an iterative, nonlinear, least

squares regression fit routine, the value of the constants K and k and a better approximation of the fatigue limit can be obtained for sets of accelerated fatigue test data, $\dot{S}$ and S_d (18,19,20).

The conventional, higher order S-N curve is completely defined by the constants m, C, and S_f. Basavaraju and Lim (10) developed relationships for m and C in terms of the parameters of the generalized Prot equation, K and k.

Basavaraju and Lim's relationships are based on the Palmgren-Miner hypothesis (4,5) of linear cumulative damage. The hypothesis states that the fatigue damage, D_i, due to n cycles at a particular stress level, S_i, is

$$D_i = \frac{n}{N} \qquad 4.8a$$

where

N = number of cycles to failure at S_i, determined from an S-N curve.

If cycling is at a number of different stress levels, the damage is summed linearly,

$$D = \frac{n_1}{N_1} + \frac{n_2}{N_2} + \ldots + \frac{n_i}{N_i} + \ldots + \frac{n_j}{N_j} = \sum_{i=1}^{j} \frac{n_i}{N_i} \qquad 4.8b$$

and failure is assumed when

$$\sum_{i=1}^{j} \frac{n_i}{N_i} = 1 \qquad 4.8c$$

By recalling the higher order hyperbolic expression for the conventional S-N curve,

$$(S-S_f)^m N = C \qquad 4.5$$

or

$$N = C/(S-S_f)^m \qquad 4.9a$$

and noting that the stress, S_i, at the ith cycle that causes damage in an accelerated fatigue test is

$$S_i = S_f + i\,\dot{S}\,, \quad i = 1, N_d. \qquad 4.10$$

4.9a can be written as

$$N_i = C/(S_f + i\,\dot{S}-S_f)^m \qquad 4.9b$$

Also, $n_i = 1$ for each cycle and 4.8b becomes

$$\frac{1}{N_1} + \frac{1}{N_2} + \ldots + \frac{1}{N_i} + \ldots + \frac{1}{N_d} = 1. \qquad 4.11a$$

Substituting 4.9b for N_i gives

$$\frac{1}{\frac{C}{(1\cdot\dot{S})^m}} + \frac{1}{\frac{C}{(2\cdot\dot{S})^m}} + \ldots + \frac{1}{\frac{C}{(i\cdot\dot{S})^m}} + \ldots \frac{1}{\frac{C}{(N_d\,\dot{S})^m}} = 1 \qquad 4.11b$$

or, by factoring $1/C/\dot{S}^m$ out,

$$\frac{\dot{S}^m}{C}\,(1^m + 2^m + \ldots + i^m + \ldots + N_d{}^m) = 1 \qquad 4.11c$$

Although there are expressions for series of natural numbers raised to an integral power, there is no constraint in this derivation that m be an integer. Basavaraju and Lim developed an expression for this series raised to a

non-integral power. By observing the terms of exact expressions of the series raised to an integral power and then comparing the value of approximations and the exact expressions, they found the approximation,

$$\sum_{j=1}^{n} j^m = 1^m + 2^m + \ldots + j^m + \ldots + n^m \approx \frac{n^{m+1}}{m+1} , \qquad 4.12$$

to be reasonably accurate. In fact, for values of n and m likely to be encountered in accerlerated fatigue testing, the error is insignificant (<<1% at n > 1000). Rewriting 4.11c in terms of the approximation, with $n = N_d$, gives

$$\frac{\dot{S}^m}{C} \frac{N_d^{m+1}}{m+1} = 1 \qquad 4.13$$

Observing that this expression can be satisfied by any set, $(\dot{S}_i, N_{d_i})$ allows for a solution for m from any two sets, $(\dot{S}_1, N_{d_1})$ and $(\dot{S}_2, N_{d_2})$:

$$\frac{\dot{S}_1^m}{C} \frac{N_{d_1}^{m+1}}{m+1} = \frac{\dot{S}_2^m}{C} \frac{N_{d_2}^{m+1}}{m+1} \qquad 4.14$$

$$m \, \mathrm{Ln}\left(\frac{\dot{S}_1}{\dot{S}_2}\right) = (m+1)\mathrm{Ln}\left(\frac{N_{d_2}}{N_{d_1}}\right)$$

$$m = \frac{1}{\frac{\mathrm{Ln}(\dot{S}_1/\dot{S}_2)}{\mathrm{Ln}(N_{d_2}/N_{d_1})} - 1} \qquad 4.15$$

This expression can be simplified by rewriting 4.1 using 4.7d, to get N_d in terms of $\dot{S}$:

$$N_d = (S_d - S_f)/\dot{S} \qquad 4.1$$

$$= (S_f + K\dot{S}^k - S_f)/\dot{S}$$

$$= K\,\dot{S}^{k-1} \quad . \qquad 4.16$$

Substituting 4.16 into 4.15:

$$m = \frac{1}{\frac{Ln(\dot{S}_1/\dot{S}_2)}{Ln\left(K\,\dot{S}_2^{k-1}/K\,\dot{S}_1^{k-1}\right)} - 1}$$

$$= \frac{1}{\frac{Ln\,\dot{S}_1 - Ln\,\dot{S}_2}{(k-1)(Ln\,\dot{S}_2 - Ln\,\dot{S}_1)} - 1}$$

$$= \frac{(k-1)(Ln\,\dot{S}_2 - Ln\,\dot{S}_1)}{-k(Ln\,\dot{S}_2 - Ln\,\dot{S}_1)}$$

$$= \frac{1-k}{k} \quad . \qquad 4.17$$

C is the only unknown left in 4.13 and it can be solved for by substituting 4.16 and 4.17:

$$\frac{\dot{S}^m}{C}\,\frac{N_d^{m+1}}{m+1} = 1$$

$$C = \frac{\dot{S}^{\left(\frac{1-k}{k}\right)}\left[K\,\dot{S}^{(k-1)}\right]^{\left(\frac{1}{k}\right)}}{\frac{1}{k}}$$

$$= k\,K^{\frac{1}{k}}\,\dot{S}^{\left(\frac{1-k}{k}\right)}\dot{S}^{\left(\frac{k-1}{k}\right)}$$

$$= k\,K^{\frac{1}{k}}\,\dot{S}^{\left(\frac{1}{k}-1+1-\frac{1}{k}\right)}$$

$$= k\,K^{\frac{1}{k}} \quad . \qquad 4.18$$

The conventional S-N curve is now completely defined (S_f,m,C) in terms of the accelerated fatigue data, S_f, K, and k.

Basavaraju and Lim conducted accelerated fatigue tests on specimens of H11 tool steel (10) and developed the conventional S-N curve from the data. The curve was compared against one obtained by conventional constant amplitude testing and they agreed reasonably well, except in the low cycle region ($< 10^4$ cycles).

In summary, there are four assumptions upon which the preceeding derivations are based: 1) the conventional S-N curve is a higher order hyperbola asymptotic to the fatigue limit and the vertical axis, 2) the accelerated fatigue S_d-N_d curve is a higher order hyperbola asymptotic to the fatigue limit and the vertical axis, 3) no damage occurs when cycling at less than the fatigue limit, and 4) Miner's cumulative damage hypothesis holds. There is evidence to support the use of the Prot method of accelerated fatigue testing and Basavaraju and Lim's extension to the theory to obtain conventional S-N curves.

Section IV: Fixture Design

4.1 Fatigue Test Fixture

In order to develop the required stress level in the anchorage rod using the available 55 kip load actuator, a "lever arm" apparatus was designed. The maximum stress level required ($S_{bar_{max}}$) was 31,000 psi in axial tension. The rods are three inches in diameter, thus the force required was,

$$\text{Force}_{req.} = (S_{bar_{max}})\ (\text{Area})$$

$$= (31{,}000)\ (7.07)$$

$$= 219{,}170 \text{ pounds}$$

$$\approx 220 \text{ kips.}$$

This was four times the capacity of the actuator, consequently, a four-to-one mechanical advantage was necessary. To ensure successful testing, a five-to-one system was designed.

A lever system (Fig. 8a) was the basis for the design, although major changes were necessary to stay within the constraints described in the introduction. The pad tie-down points are not capable of reacting large moments, which led to the use of a self-equilibriating system. This system (Fig. 8b) allowed the tensile force generated in the bar to be reacted parallel to it through large side beams in compression. The force was transferred to the

a.

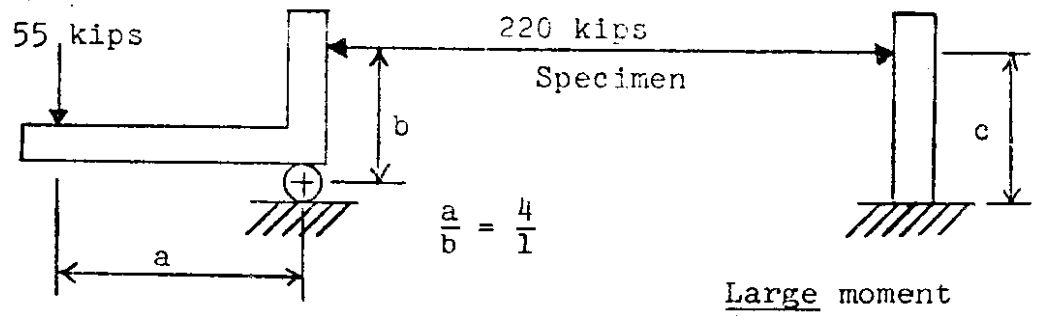

Large moment
(220 × c ft-lbs)
reacted here
at tie-down.

b.

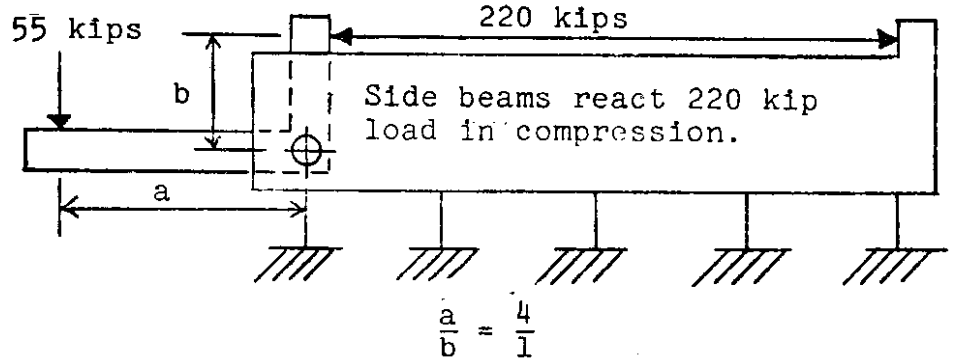

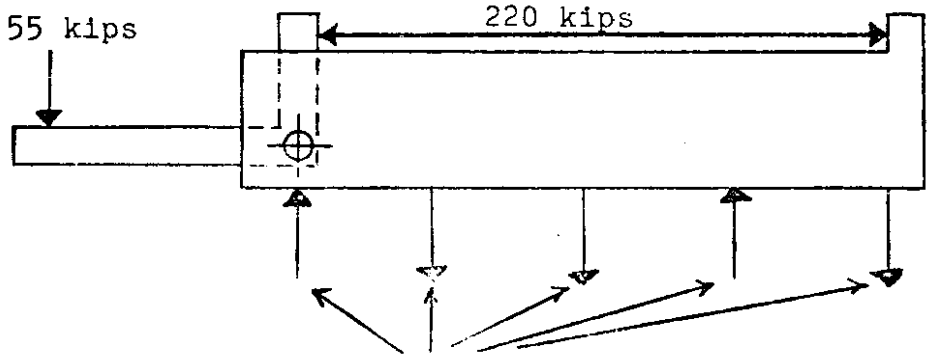

Loads reacted in tension or compression
with small moments.

Fig. 8 TEST FIXTURE DESIGN SCHEMATICS

side beams through a very stiff end plate (moment) connection at one end and a high strength steel (AISI 4330M) pin at the other end. The entire mechanism then acted, in effect, as a large, rigid beam. Only the load applied by the actuator had to be reacted at the pad tie-downs. These reactions were tensile and compressive with some small moments and were within the capability of the tie-downs (25 kips in tension). The mechanism is depicted in Fig. 8c.

The test pad itself was pre-stressed concrete, rectangular in plan and 12 inches in depth. The dimensions were 20 feet, 10 inches by 8 feet with 21 threaded tie-downs on 36 inch centers.

The materials available for construction consisted mainly of various thicknesses of steel plate and a small selection of beams, ranging in section from W8 to W18. These pieces were all ASTM A36 steel. The Structures Laboratory also maintains a selection of angles, bars, sheet, etc. of assorted materials and sizes. It is important to recall that the specimens were to be tested full-sized and that the pad is not much longer than the specimen itself.

The primary design concern, aside from reacting the load and safely storing the large amount of strain energy generated by the rod, was to prevent fatigue failures of the fixture while testing. Components were sized so as to

keep stress levels as low as possible. The fatigue limit (R = -1) of A36 steel is on the order of 18,000 psi and was chosen as the maximum allowable net section stress for A36 members. There were a few areas where the net section stress could not be held under 18,000 psi due to the sizes of material available and these areas were monitored closely during testing. Most of these areas were confined to the lever arm connection to the side beams. Local reinforcement was added at stress concentrations such as corners, cutouts, etc., where feasible. The fixture is shown in Fig. 9.

All assembly was done by welding. The high strength steel pin around which the lever rotates was a press fit. The specimen was attached with a threaded nut and washer at one end and with a self-aligning nut and washer assembly at the lever arm end, to prevent bending. Although the rotation at the pin at maximum load was only 2.19 degrees (Appendix B), the self-aligning nut assembly ensured that the bar would be free from the effects of out-of-plane bending. Recall that failure was not expected to occur at the center of the rod where any effects of bending would be most pronounced. Failure was expected in the threaded portion where effects of bending would be secondary. The self-aligning nut assembly is shown in Fig. 10a.

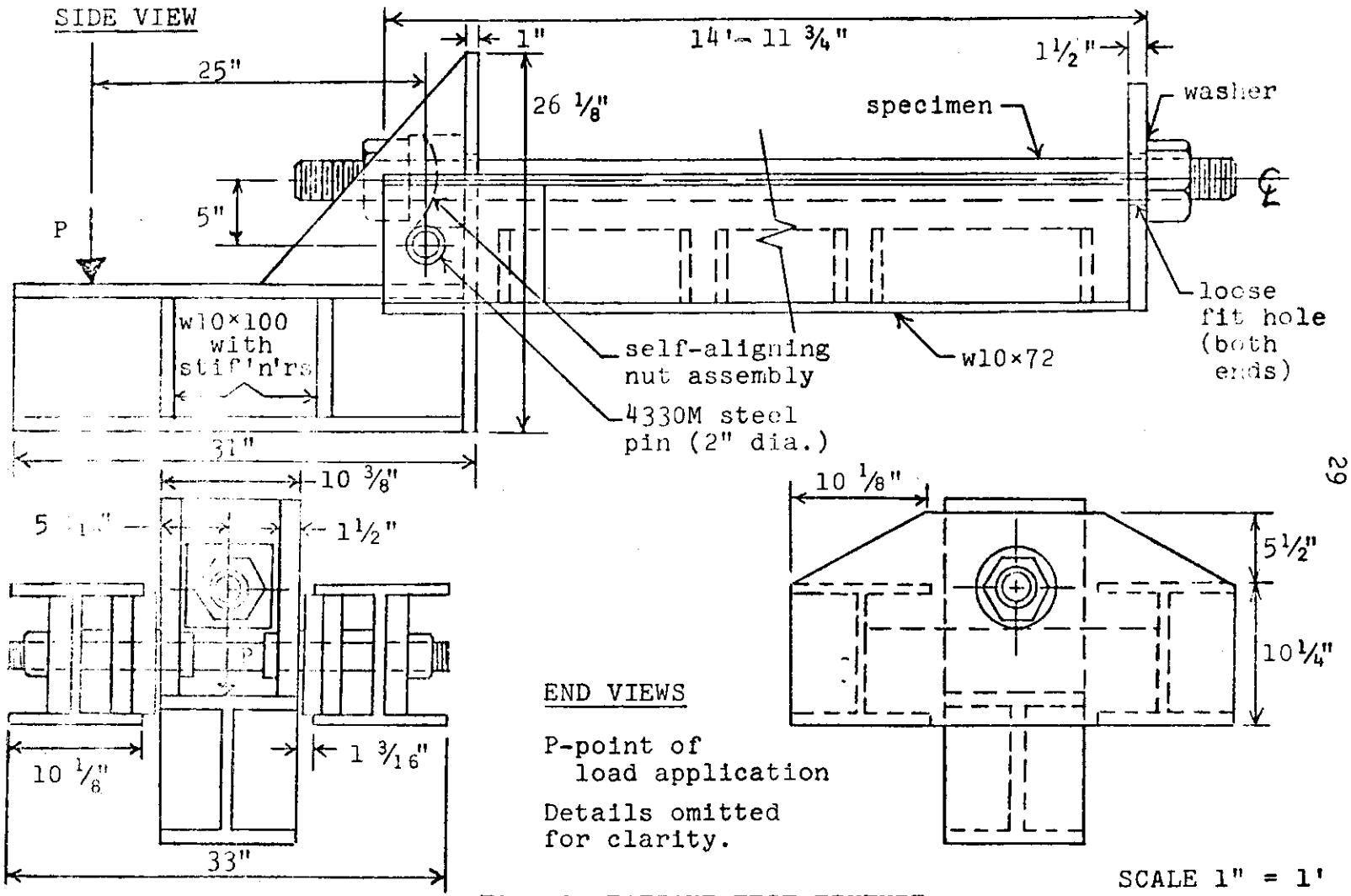

Fig. 9 FATIGUE TEST FIXTURE

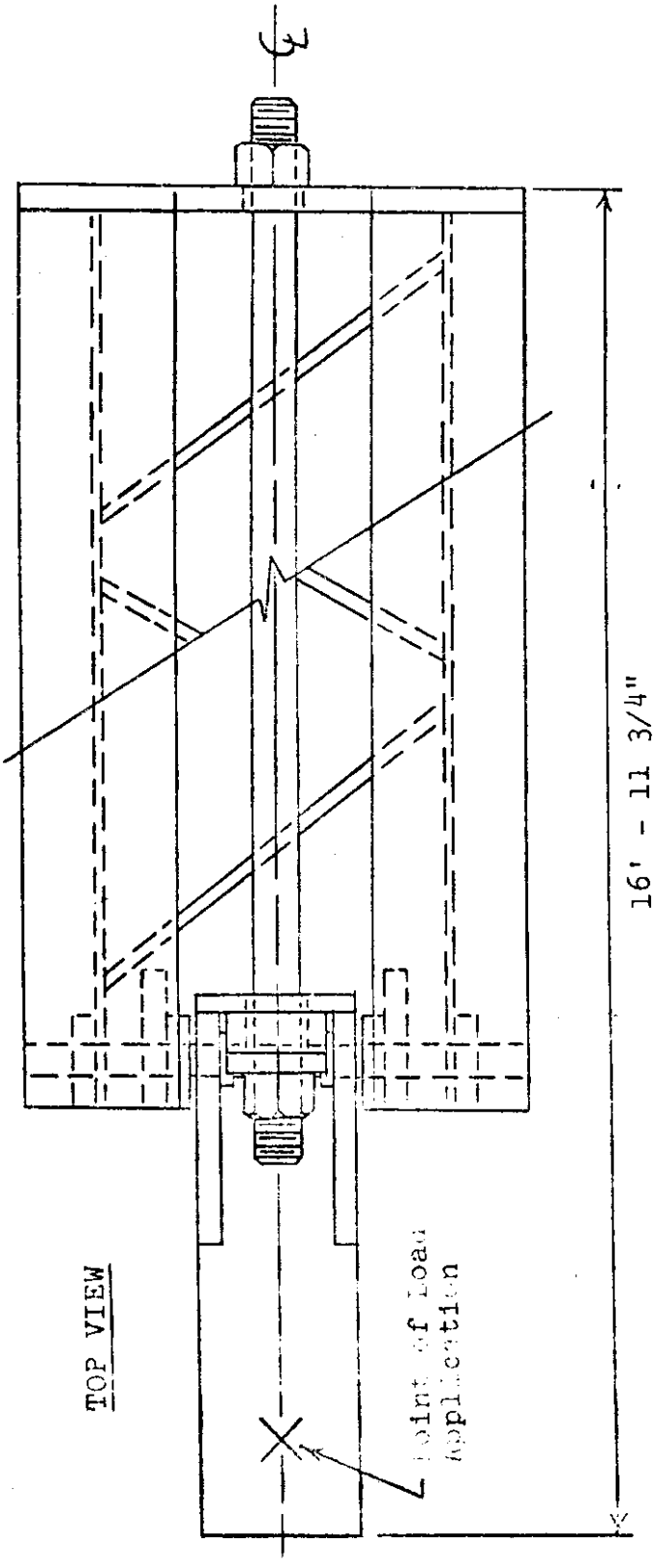

Fig. 9 FATIGUE TEST FIXTURE

Fig. 9 FATIGUE TEST FIXTURE

a. Self-aligning nut assembly

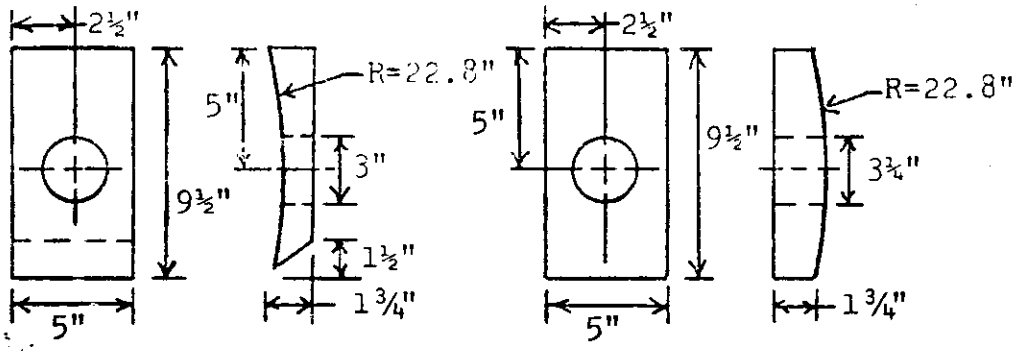

b. Tie-down detail

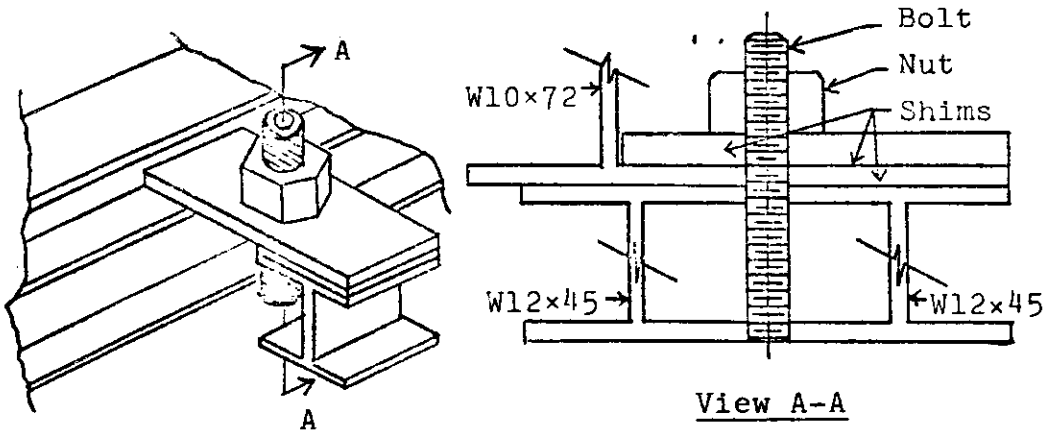

c. Actuator frame

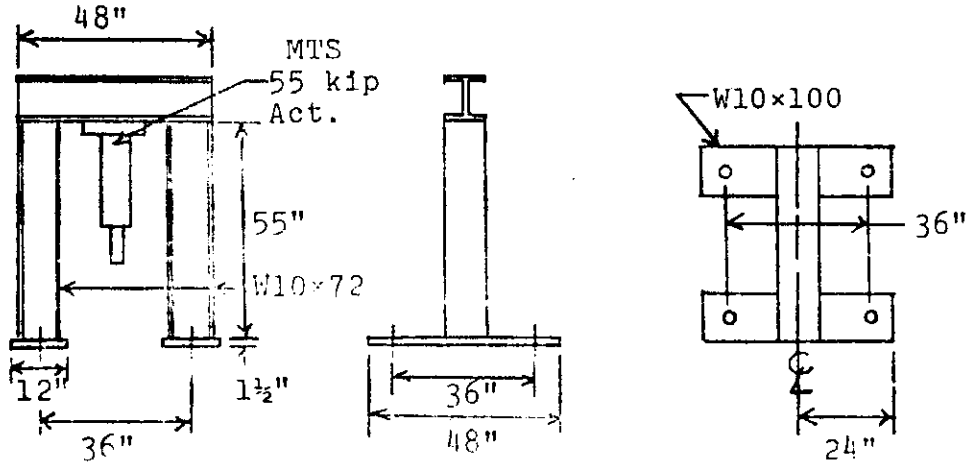

Fig. 10 TEST FIXTURE DETAILS

The fixture was attached to the pad by clamping the flanges of the side beams down on pieces of steel beam at ten points. A cut-away of a tie-down is shown in Fig. 10b. Analysis of the mechanism for the reactions into the pad was carried out using the displacement method of structural analysis (Appendix C). Reactions were found to be within the capability of the pad.

4.2 Actuator Frame and Attachment

The actuator was bolted upside down to a simple inverted "U" framework (Fig. 10c). The frame reacted the actuator load in tension through four tie-downs.

The actuator was attached to the lever arm using a simple swivel mechanism that provided rotational movement in a fore and aft direction. The base of the actuator was also on a fore and aft swivel platform. This arrangement ensured freedom from binding during loading.

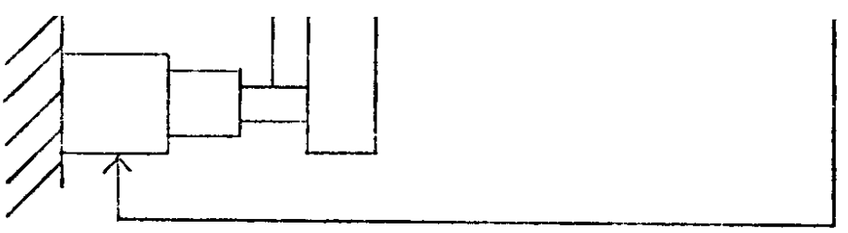

Fig.

Fig. 12 FAILURE SURFACES

Fig. 12 FAILURE SURFACES

linearly with respect to cycle (i.e., load), was more than an order of magnitude less than the axial strain. Further, the crack initiation zones on the failure surfaces (Fig. 12) tended to assume a "crescent" shape, characteristic of tension-tension or tension-compression fatigue testing. Bending fatigue normally results in an "arc"-shaped crack initiation zone, with a flat bottom which translates across the failure surface during cycling. The effects of bending were assumed to be insignificant at the rod ends.

Initial testing showed that galling of the bearing surfaces on the lever arm pin and grip assemblies was allowing transfer of moment to the side beams and, in turn, undesirable deflections of the fixture. Fittings were added to these assemblies so that anti-seize compounds could be continually added. No further galling was noted.

The test results were used as data for a non-linear, least squares regression analysis routine (22) to fit an equation of the form

$$y = C_1 + C_2 \, x^{C_3} \qquad 6.1$$

by evaluation of the constants C_1, C_2, and C_3. These correspond to the constants S_f, K, and k in the generalized Prot relationship (Eq. 4.7d). The equation determined from the data was

where the fatigue limit is 16484 psi. Eq. 6.2 is plotted with the experimental data in Fig. 13.

Computation of m and C, using the relations developed in Section 3.3, results in the equation for a conventional S-N curve:

$$\cdot\ S_d = 16484 + 6280\ \dot{S}^{.6342}$$

$$\cdot\ S_f = 16484 \text{ psi}$$

$$\cdot\ m = \frac{1 - .6342}{.6342} = .5768$$

$$\cdot\ C = (.6342)(6280)^{1/.6342} = 617{,}746$$

$$\cdot\ (S - 16484)^{.5768}\ N = 617{,}746$$

This curve is shown in Fig. 14.

In summary, it is evident that the Prot method of accelerated fatigue testing, coupled with Basvaraju and Lim's relationships, have allowed the determination of the S-N curve from a small number of specimens and in a short amount of time. A conventional, constant amplitude test program would likely have taken at least an order of magnitude more time.

Additionally, Floating Bridge failures have been duplicated in the laboratory and, thus, the S-N curve may now be used in cumulative damage analyses for prediction of anchorage rod failures. It may be assumed that the S-N curve is conservative due to the condition of the specimens at the start of the test. That is, the unknown length of time in service prior to testing and corrosion processes

Figure 13

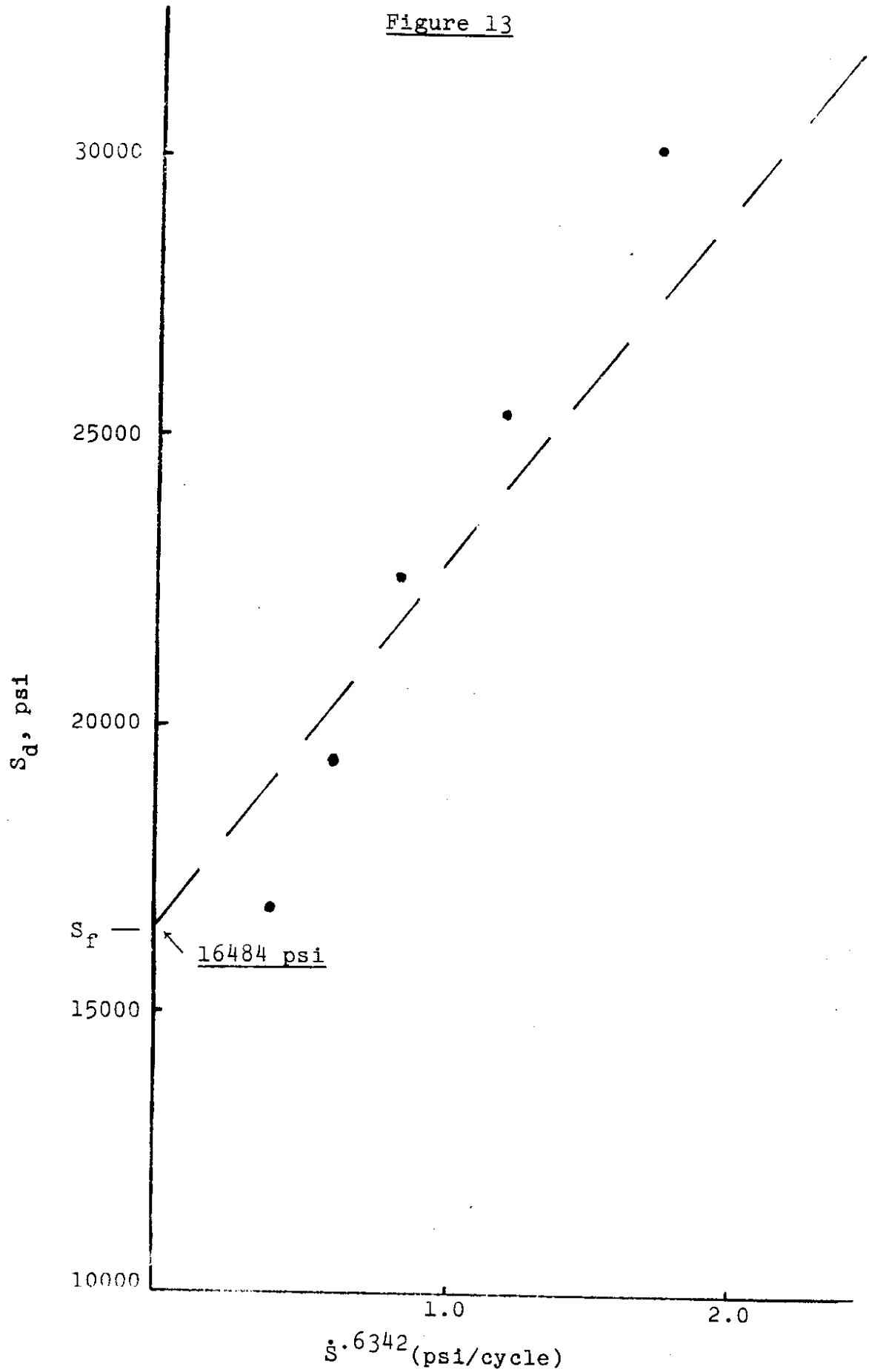
30000
25000
20000
S_f
15000
10000
S_d, psi
16484 psi
1.0
2.0
$\dot{S}^{.6342}$ (psi/cycle)

during service and subsequent storage may have induced the formation of incipient fatigue cracks before the test started.

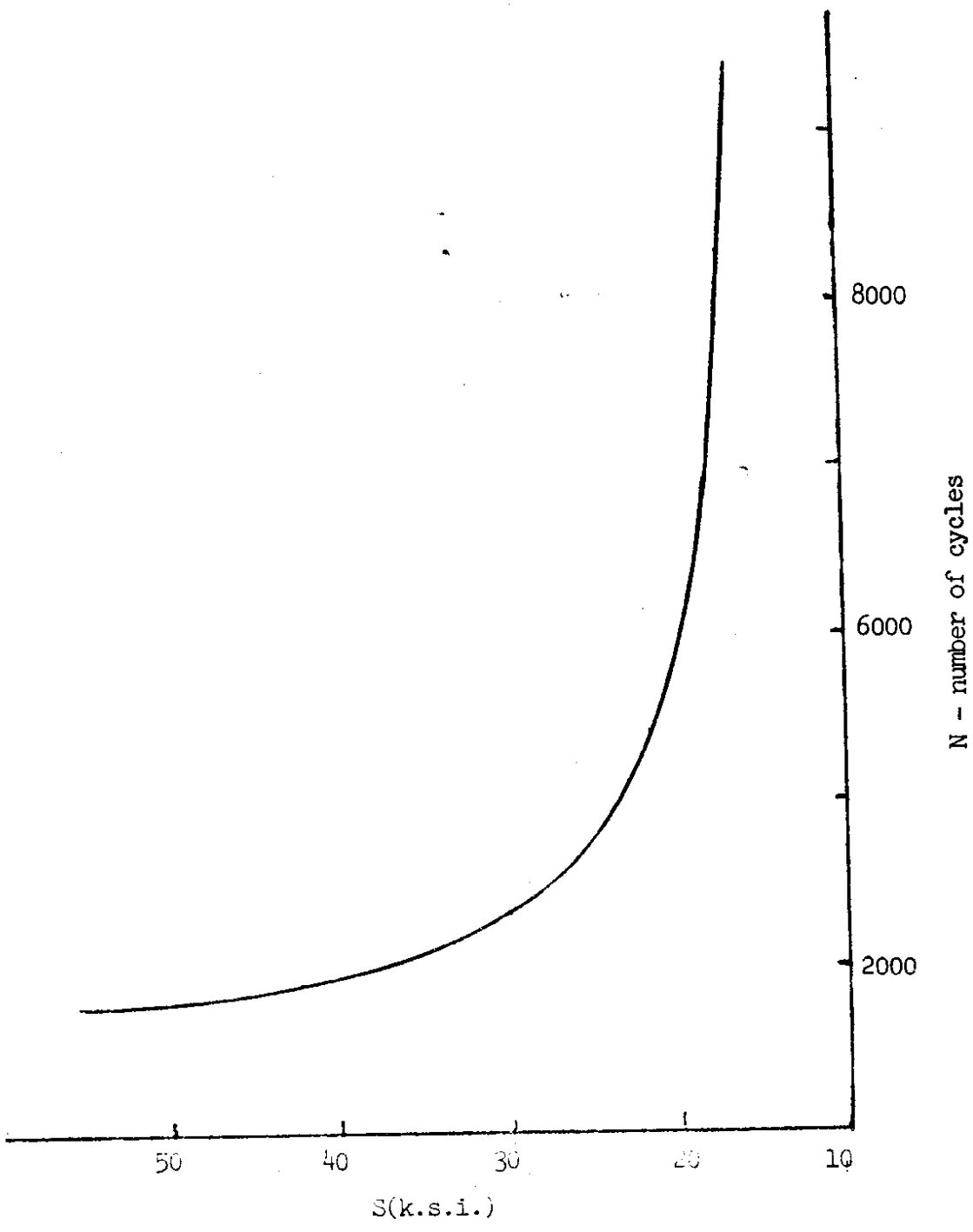

Figure 14

Section VII: Conclusions

1. The feasibility of full-scale testing of vertical trunnion anchorage rods within the bounds of given constraints has been demonstrated.

2. Duplication of Floating Bridge failure modes was achieved.

3. Evidence is available to support the use of the Prot method of accelerated fatigue testing and Basavaraju and Lim's extension to develop the conventional S-N curve from Prot data.

4. A conservative estimate of the S-N curve for vertical trunnion anchorage rods has been developed.

5. Accelerated fatigue testing results in a large reduction in test time as compared to that required for conventional, constant amplitude testing.

6. A test fixture has been designed that could be used for other fatigue or static strength testing of large specimens, with modifications as required: structural reinforcement where necessary, suitable grip design, and compression restraints, if necessary.

Section VIII: References

1. Brown, C., Christensen, D., and Demich, G. "Evergreen Point Bridge Maintenance Problems," Methods of Structural Analysis, Vol. I, Proceedings of the National Structural Engineering Conference, ASCE, 1976, pp. 189-203.
2. Bright, A. "Comparison of Fatigue Theories and Design Recommendations for Fatigue," Master of Science Thesis, University of Washington, 1977.
3. Vasu, R. "A Study of the Fatigue of a Component of the Evergreen Point Bridge Drawspan," Master of Science Thesis, University of Washington, 1977.
4. Palmgren, A. "Die Lebendauer von Kugellagern," Zeitschrift des Vereines, Deutsches Ingeneure, Vol. 68, No. 14, 1924, pp. 339-341.
5. Miner, M. "Cumulative Damage in Fatigue," Transactions of the ASME, Vol. 67, 1945, pp. A159-164.
6. Juvinall, R. Engineering Considerations of Stress, Strain and Strength, McGraw-Hill Book Co., 1967.
7. Osgood, C. Fatigue Design, Wiley-Interscience, 1970.
8. Sandor, B. Fundamentals of Cyclic Stress and Strain, University of Wisconsin Press, 1972.
9. Prot. E. "Fatigue Testing under Progressive Loading, a New Technique for Testing Materials," Review de Metallurgie, 45, 1948, pp. 481-489. (Translated by [illegible], E., WADC-TR-52-148, 1952.

10. Basavaraju, C., and Lim, C. "An Analytical Approach to Determine Conventional S-N Curves from Accelerated-Fatigue Data," Experimental Mechanics, Vol. 17, No. 10, Oct., 1977, pp. 375-380.

11. Report of Chemical and Physical Test, Cardinal Foundry and Power Supply, Cleveland, Ohio, 18 August, 1976.

12. Modern Steels and Their Properties, 6th Edition, Bethlehem Steel Co., Bethlehem, Penn., 1961, pp. 122-123.

13. Lee, H., and Uhlig, H. "Corrosion Fatigue of Type 4140 High Strength Steel," Metallurgical Transactions, Vol. 3, Nov., 1972, pp. 2949-2958.

14. Metals Handbook, 8th Edition, Vol. 1, American Society for Metals, Metals Park, Ohio, 1961, pp. 217-224.

15. Handbook of Fatigue Testing, ASTM STP 566, Swanson, S., Editor, American Society for Testing and Materials, 1974.

16. Peterson, R. Stress Concentration Factors, John Wiley and Sons, New York, 1974.

17. Corten, H., Dimoff, T., and Dolan, T. "An Appraisal of the Prot Method of Fatigue Testing," Proceedings of the American Society of Testing and Materials, Vol. 54, 1954, p. 875.

18. Diez, J., and Salkin, R. "Appraisal of the Locati and Prot Methods for Determining Fatuge Limits," Journal of Materials, JMLSA, Vol. 7, No. 1, March, 1972, pp. 32-37.

19. Lim, C., and Thorne, D. "An Accelerated Fatigue Model," ASME Paper 74-DE-18, American Society of Mechanical Engineers, April, 1974.

20. Lim, C., and Kuklentz, R. "Application of the Digital Computer to an Accelerated Fatigue Model," Use of Computers in the Fatigue Laboratory, ASTM STP 613, Mindlen, H., and Langraf, R., Eds., American Society for Testing and Materials, 1976, pp. 126-141.

21. Metals Handbook, 8th Edition, Vol. 3, American Society for Metals, Metals Park, Ohio, 1974, p. 32.

22. Robinson, B. "SPSS Subprogram NONLINEAR-Nonlinear Regression," University of Washington Academic Computer Center Announcement #26, February, 1978.

Appendix A

Calculation of thread root stress concentration factor and fatigue notch factor

For 3-4 UNC 2A thread

D = outside diameter

= 3.0 in., and

K = root diameter

= 2.675 in.

There are four threads per inch, thus

P = pitch = 1/4

= .25.

The theoretical width, W_T, at the flat of the thread root is

$$W_T = P/8 = .25/8$$

$$= .03.$$

Assume the best machining practice results in an actual root width, W_A, of

$$W_A = W_T/2 = .03/2$$

$$= .015.$$

Calculate the ratios:

$$\frac{W_A}{K} = \frac{.015}{2.675}$$

$$= .006$$

and

$$\frac{K}{D} = \frac{2.675}{3.000} = .892$$

From Peterson (16), Fig. 31, for these ratios, the stress concentration factor is

$$K_T = 5.7.$$

The fatigue notch factor, K_f, is calculated using

$$K_f = 1 + q(K_T - 1)$$

where

q = notch sensitivity factor.

Peterson, Fig. 8, shows q for this type of steel to be

$$q = .8,$$

and, therefore,

$$K_f = 1 + .8(5.7 - 1)$$

$$= 4.8.$$

Appendix B

Calculation of displacements and rotations at lever arm

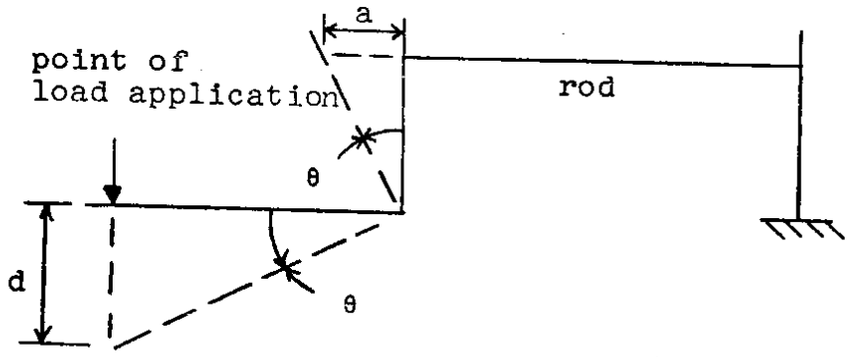

a = rod elongation

d = actuator piston displacement (stroke)

θ = lever arm rotation

The stress, S, required in the rod is,

S = 31,124 psi.

The modulus of elasticity, E, for this material is,

$E = 31.25 \times 10^6$ psi,

and the maximum strain, e, in the rod is

$e = S/E = 31,124/31.25 \times 10^6$

$= 9.96 \times 10^{-4}$ in

= 996 μs.

The total elongation, a, assuming the rod is 16 ft. long, is

$a = (\text{length})(e) = (16)(12)(9.96 \times 10^{-4})$

= .191 in.

The rotation, θ, of the lever arm is

$$\theta = \sin^{-1}(a/5.0) = \sin^{-1}(.191/5.0)$$
$$= \sin^{-1}(.0382)$$
$$= 2.19°.$$

The stroke, d, required is,

$$d = 25 \sin \theta = 25 \sin(2.19°)$$
$$= .956 \text{ in.}$$

Appendix C

Calculation of Pad Tie-Down Reactions

Determination of the reactions in the tie-downs was carried out using the displacement method of structural analysis. Calculations were performed using the SMIS (Symbolic Matrix Interpretive System) computer program maintained on the University of Washington academic computer system.

Due to symmetry, only one half of the structure was modelled. The lever arm and side were assumed to be rigidly connected at the pin. Member and node numbering and member properties are shown in Fig. C1. Member ten is representative of a six-inch section of the W12x45 support rail upon which the fixture lays. It was assumed to be the support about which the structure will try to rotate.

Bending moment and axial force diagrams are shown in Fig. C2. Note that the highest tensile load in a reaction member is 14,443 lbs., within the 25,000 lbs. capability of the pad.

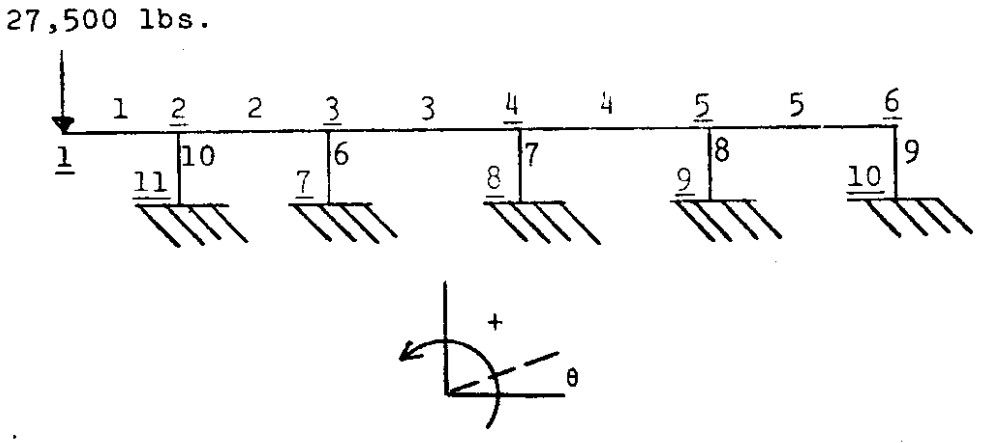

i, node number (11 total nodes)

i, member number (10 total members)

Member	θ	Length (in)	E (psi)	I (in^4)	A (in^2)	A_{shear} (in^2)
1	0	25	30×10^6	625	29.43	8.34
2	0	29	30×10^6	420.7	21.18	5.25
3-5	0	36	30×10^6	420.7	21.18	5.25
6-9	π/2	12.25	30×10^6	3.98	7.07	6.36
10	π/2	12.25	30×10^6	6.75	2.25	4.59

Fig. C.1 STRUCTURE MODEL AND MEMBER PROPERTIES

Bending moment (in-lbs), numbers plotted on compression side.
(Members separated for clarity).

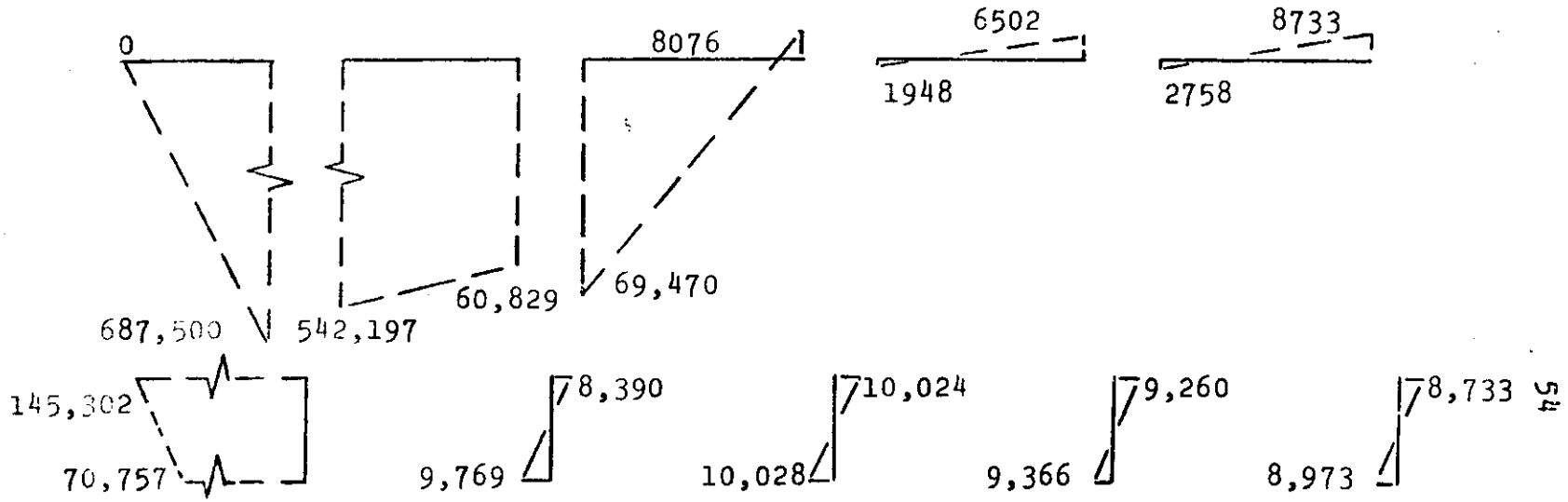

Axial force (lbs.), → ← compression - ← → tension

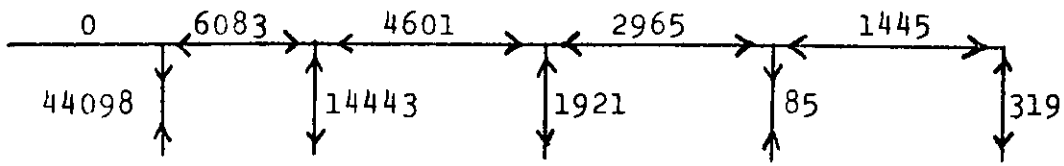

Fig. C.2 BENDING MOMENT AND AXIAL FORCE DIAGRAMS

VALIDITY OF MINER'S LAW

So much of the work in this project was based on the validity of Miner's cumulative damage law. In order to examine this law, Mr. Ade Bright compared it with seven other theories. The comparison was by examining the fit of these theories to available test data. His conclusion is that Miner's theory is the simplest and is in no way less valid than the others. By the application of Occam's Razor, the use of Miner's theory is justified. Again, the original numbering of the thesis is retained.

TABLE OF CONTENTS

LIST OF TABLES

LIST OF FIGURES

NOTATIONS

Symbols

D	=	Total damage
$\overline{D}$	=	Average damage
ΔD	=	Damage increment
E	=	Modulus of Elasticity
E_k	=	Expectation
H	=	Entropy
K	=	Experimental constant
L	=	Crack length at any stage
L_o	=	Griffith's crack length
M	=	Mean
N	=	Fatigue life
N_F	=	Number of cycles to failure
N_R	=	Reference fatigue life
N'	=	Modified life
N''	=	Number of cycles to initiate crack
N'''	=	Number of cycles to propagate crack to failure
P	=	Probability
R	=	Reliability
RMS	=	Root mean square
S	=	Alternating stress amplitude
S_E	=	Endurance limit

S'_E = New endurance limit

$S_{E,i}$ = Endurance limit at i^{th} stress application

$S_{i,min}$ = Minimum stress

S_R = Reference stress

S_u = Ultimate strength

S_y = Yield strength

ΔS = Stress increment

T_F = Time to failure

V = Variance

a = Experimental constant

b = Slope parameter of conventional S-N curve

c = Material constant for virgin material

c' = Material constant for stressed material

d = Cycle ratio or damage

g = Entropy function

ksi = Units of stress (thousands of pounds per square inch)

n = Applied number of cycles

n^* = Partial cycles

s = Standard deviation

α = Fraction of applied cycles in block or variable stress loading

Γ = Gamma function

δ = Slope parameter of modified or fictitious S-N curve

λ = Lagrangian multiplier

ν_o^*	=	Number of zero crossings with positive slope of random stress history
ξ	=	Stress interaction factor
σ	=	RMS
$\sqrt{2}\sigma$	=	Peak stress in random loading
erf	=	Error function

ACKNOWLEDGEMENT

The writer expresses his sincere gratitude and appreciation to Dr. Colin B. Brown for his guidance and moral support throughout this work, special thanks to Dr. Neil Hawkins and Dr. William Miller for their assistance as members of the Examination Committee. Also, special thanks is extended to the State Highway Department for financial assistance. Appreciation to Merrill Little who did all of the typing, and last but not least great appreciation to my wife for her patience and encouragement.

1. INTRODUCTION

In recent years, a number of cumulative fatigue damage theories have been proposed. These theories are based on the effects of the application of a sequence of varied load amplitudes on the fatigue life of metals. In general, these theories can be classified as (a) stress-independent and (b) stress-dependent.

Stress-independent theories assume damage dependency on cycle ratio only. Here we define cycle ratio as the quotient of number of cycles applied divided by the number of cycles to failure at the same stress amplitude. Hence the same amount of damage is done by equal cycle ratios, regardless of stress amplitudes. This is illustrated in Fig. 1. On the other hand, stress-dependent theories are sensitive to the magnitude of stress amplitudes. Thus damage is defined not only by the cycle ratios but also by the number of applied stress amplitudes as shown in Fig. 2. Experiments are necessary to evaluate this stress-dependency.

The various damage calculation methods give only estimates of life prediction required for structural designs. It is intended therefore, to make quantitative comparisons of some damage theories, with more emphasis on the Miner's theory, within the limitations of available data.

Before entering into this discussion, it is necessary to define the types of stress loading history used here.

1.1 Step Test (Prestress Test): Specimen is subjected to one or more successive stress levels, S_1, S_2, S_3, ..., S_i for a corresponding predetermined number of cycles, n_1, n_2, n_3, ..., n_i (where $n_k < N_k$, the number of cycles to failure) then tested to failure at some other stress level, S_{i+1}.

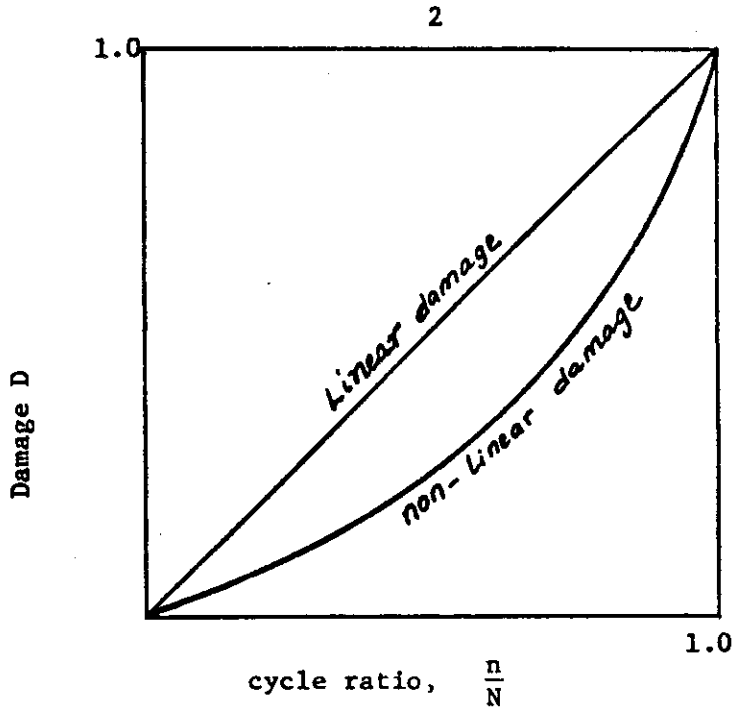

FIG. 1 SCHEMATIC REPRESENTATION OF STRESS-INDEPENDENT DAMAGE THEORY

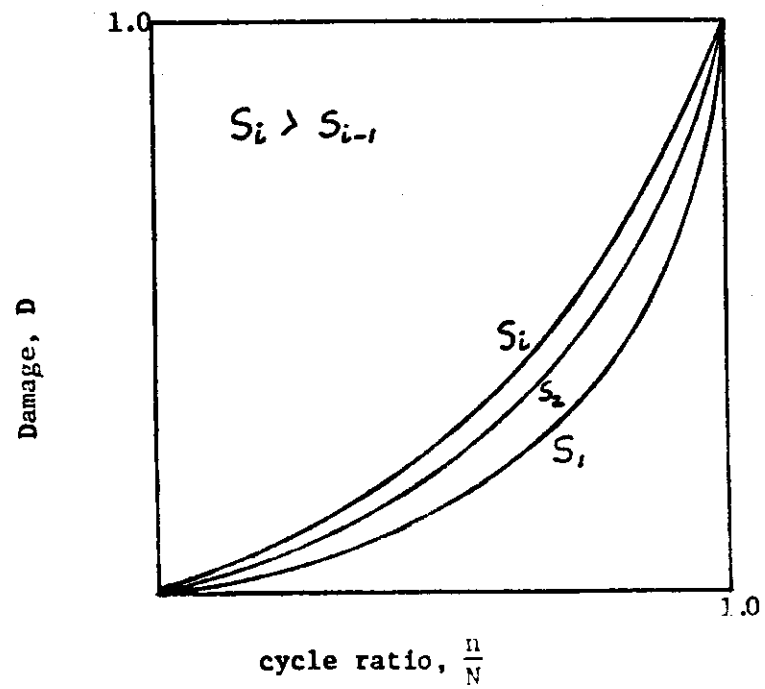

FIG. 2 SCHEMATIC REPRESENTATION OF STRESS-DEPENDENT DAMAGE THEORY

This is illustrated in Fig. 3, for i = 2.

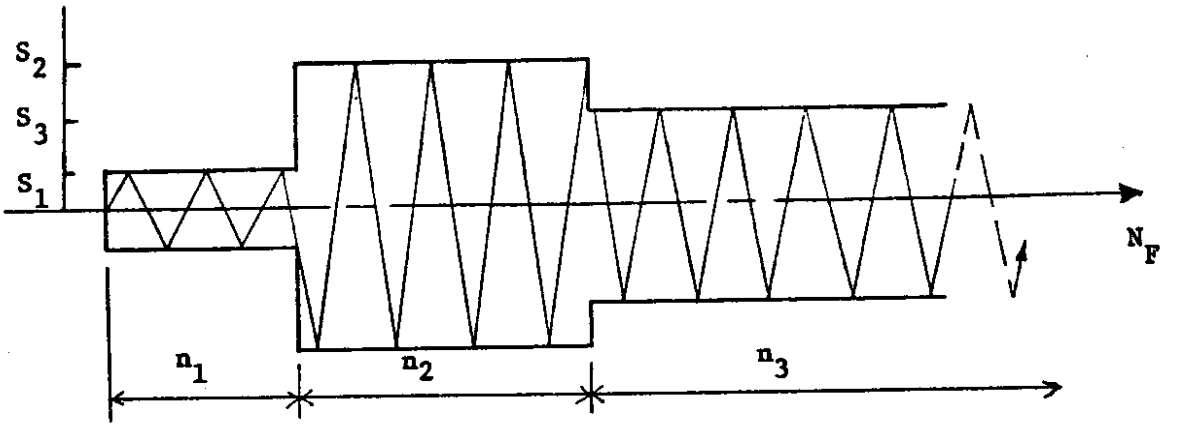

FIG. 3 THREE-STEP PRESTRESS LOADING HISTORY

1.2 Repeated Multi-Level Stress Loading (block loading): Specimen is tested repeatedly at two or more stress levels, S_1, S_2, S_3,.., S_i, for fixed number of cycles, n_1, n_2, n_3, ...,n_i respectively, in the same sequence until failure. In this case, $S_1 > S_2 > S_3 > .. > S_i$ and n_1, n_2, n_3, ..., n_i are fractions of a cycle block. This block is shown in Fig. 4 for i = 3.

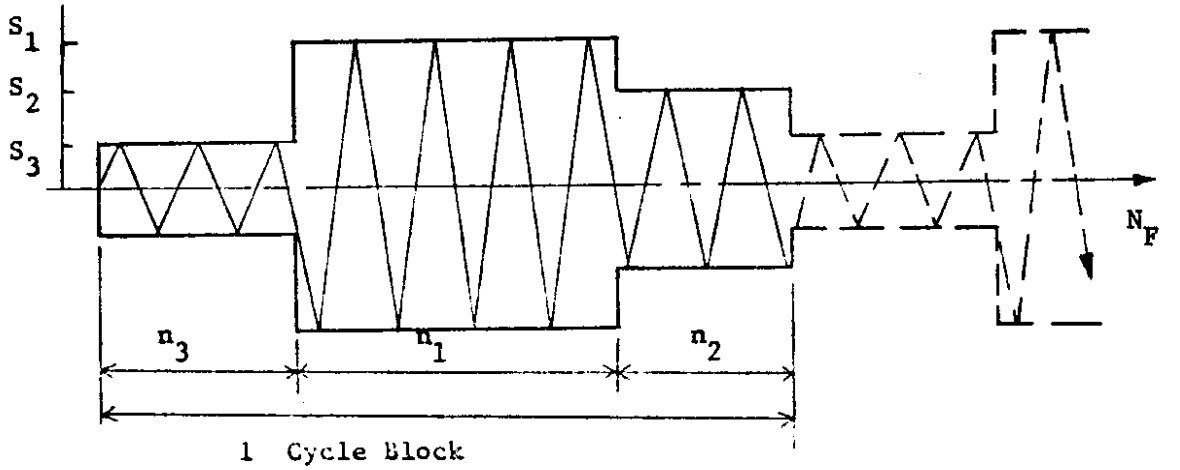

FIG. 4 BLOCK LOADING HISTORY

1.3 Random Multi-Level Stress Loading: Same as (1.2) but the sequence of the stresses is randomly applied within each block.

1.4 Continuously Varying Stress Loading: Specimen is subjected to a stress pattern applied in some geometric form (i.e. Sine wave, exponential pattern, etc.) as shown in Figs. 5a and 5b, until failure. In this case S_1 is the maximum stress.

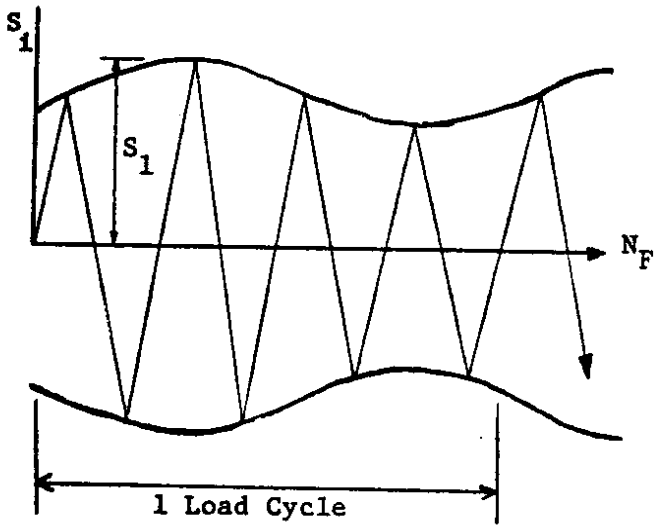

FIG. 5a SINE WAVE LOADING HISTORY

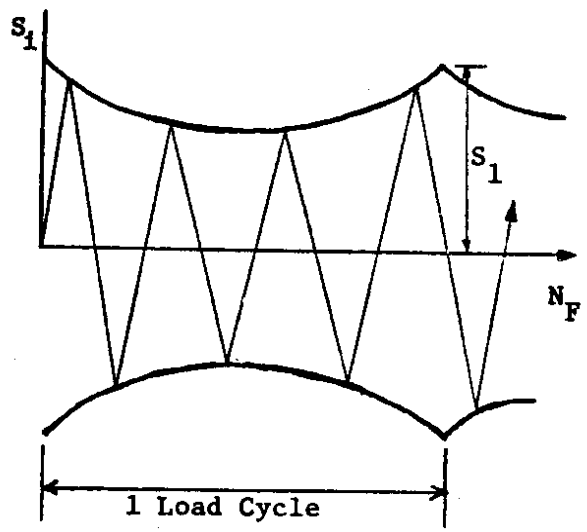

FIG. 5b EXPONENTIAL LOADING HISTORY

1.5 Random Loading: Each stress cycle is randomized by the use of random noise generators or other sources of random input.

2. REVIEW OF SOME DAMAGE THEORIES

This section reviews some of the theories employed in fatigue predictions. In a later part, the Miner, Henry, Manson, Valluri and Freudenthal theories are compared in the light of available data. Unfortunately, such data does not make available essential parameters necessary for the use of the other theories.

2.1 Miner's Theory (1): Commonly referred to as the linear damage rule, is the most widely use in fatigue design estimation because of its simplicity. It serves as basis for the derivation of a number of fatigue damage theories.

Damage is defined as

$$d_i = \frac{n_i}{N_i} \tag{2-1}$$

where n_i = number of applied cycles at stress, S_i

N_i = number of cycles to cause failure under constant amplitude stress, S_i

and failure occur when damage reaches unity.

This is represented by

$$D = \sum_{i=1}^{k} d_i = 1.0 \tag{2-2a}$$

or

$$\sum_{i=1}^{k} \frac{n_i}{N_i} = 1.0 \tag{2-2b}$$

This relat nship is shown in Fig. 6.

2.1.1 Under Prestress Loading: For Prestressed conditions remaining life after $(i - 1)^{th}$ prestress is obtained by the use of eq. (2-2b), thus

$$n_i = N_i \left(1 - \frac{n_1}{N_1} - \frac{n_2}{N_2} - \cdots - \frac{n_{i-1}}{N_{i-1}}\right) \qquad (2\text{-}3)$$

2.1.2 Under Block Loading: As defined earlier, (see Fig. 4) let

$$\frac{n_i}{N_F} = \alpha_i \qquad (2\text{-}4a)$$

or

$$n_i = \alpha_i N_F \qquad (2\text{-}4b)$$

where α_i = cycle ratio under stress S_i

The substitution of eq. (2-4b) into (2-2b) yields

$$\sum_{i=1}^{k} \frac{\alpha_i N_F}{N_i} = 1.0 \qquad (2\text{-}5)$$

Number of cycles to failure under this condition is therefore

$$N_F = \frac{1}{\sum_{i=1}^{k} \frac{\alpha_i}{N_i}} \qquad (2\text{-}6)$$

From a linear log - log plot of the S-N diagram

$$N_i = N_R \left(\frac{S_R}{S_i}\right)^b \qquad (2\text{-}7)$$

where b = inverse slope of the best fit line

S_R = reference stress

N_R = reference life corresponding to S_R

S_R and N_R can be taken as S_1 and N_1 respectively, noting as stated earlier that S_1 is the maximum peak stress under this condition.

Thus

$$N_F = \frac{1}{\sum_{i=1}^{k} \frac{\alpha_i}{N_1(\frac{S_1}{S_i})^b}} = \frac{N_1}{\sum_{i=1}^{k} \alpha_i(\frac{S_i}{S_1})^b} \qquad (2\text{-}8)$$

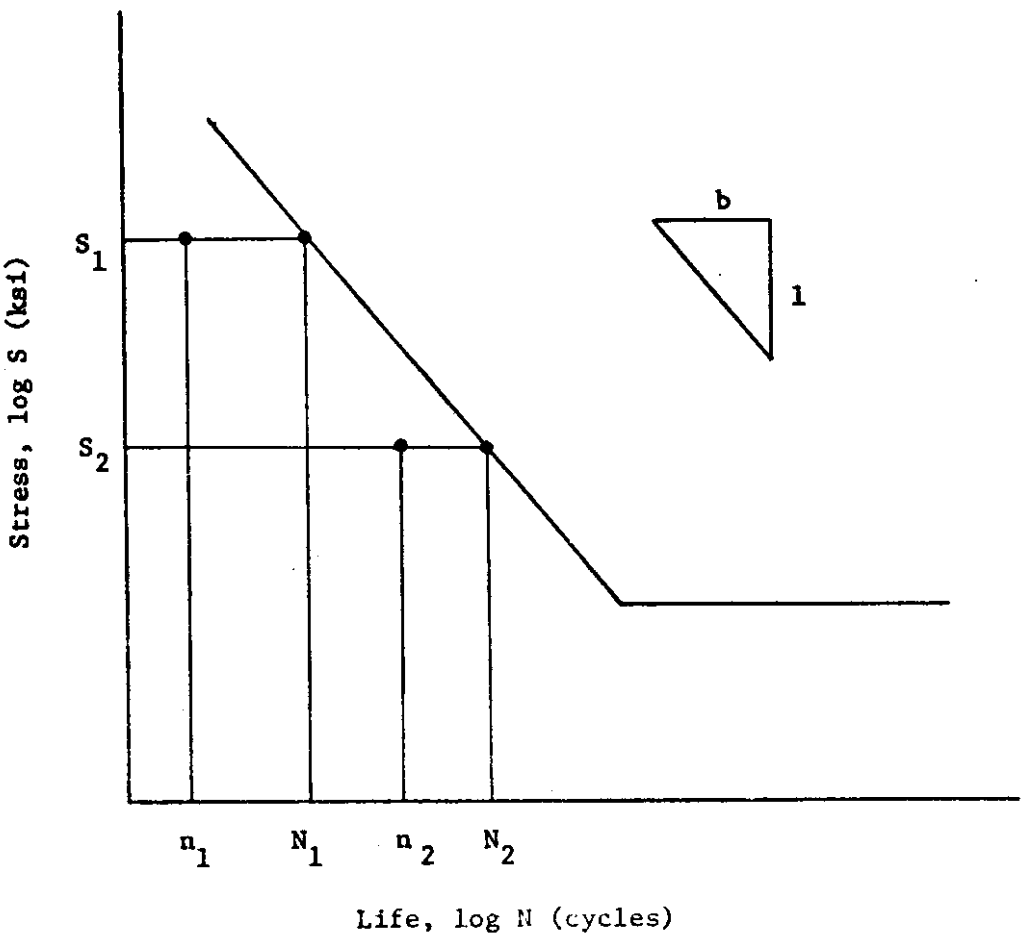

FIG. 6 REPRESENTATION OF MINER'S RULE

2.1.3 Under Continuously Varying Stress Loading: The relationship given in eq. (2-8) does hold for this condition. In order to evaluate the various continuous stresses, S_i it is necessary to break the stress history in a load cycle into discrete parts made of small intervals, ΔS. Thus the cycle ratios, α_i can be calculated by summing the number cycle per unit load cycle within the range $S_i + \Delta S$, whose average value is taken as $\overline{S}_i$. Consequently, eq. (2-8) becomes

$$N_F = \frac{N_1}{\sum_{i=1}^{K} \alpha_i \left(\frac{\overline{S}_i}{S_1}\right)^b} \tag{2-9}$$

2.1.4 Random Fatigue Life Prediction (Miner-Rayleigh): For a stationary narrow-band random process, P(S) is the probability of peaks between S and S + ΔS and the number of cycles occurring per unit time between those peak stress is n(S) dS, therefore total number of cycles per unit time of all peak stresses is given as

$$N_F = \int_0^\infty n(S)\, dS \tag{2-10}$$

where $n(s) = \nu_o^* T_F P(S)\, dS = N_F P(S)\, dS$

ν_o^* = number of zero crossings with positive slope

T_F = time to failure

Redefining damage in eq. (2-1) as

$$d_i = \frac{n(S_i)}{N(S_i)} \tag{2-11a}$$

or

$$d_i = N_F \frac{P(S_i)dS}{N(S_i)} \tag{2-11b}$$

under the above conditions, peak stresses follow Rayleigh distribution given by

$$P(S) = \frac{S}{\sigma^2} \exp[-\tfrac{1}{2}(\frac{S}{\sigma})^2] \tag{2-12}$$

Substituting eq. (2-12) into eq. (2-11b)

total damage,

$$D = N_F \int_o^\infty \frac{P(S)}{N(S)} dS$$

$$= N_F \int_o^\infty \frac{S_i}{\sigma_i^2} \frac{1}{N(S_i)} \exp[-\tfrac{1}{2}(\frac{S_i}{\sigma_i})^2] \, dS_i \tag{2-13}$$

Using the relationship in eq. (2-7)

$$D = N_F \int_o^\infty \frac{S_i}{\sigma_i} \frac{1}{N_R}(\frac{S_i}{S_R})^b \exp[-\tfrac{1}{2}(\frac{S_i}{\sigma_i})^2] \, dS_i$$

$$= \frac{N_F}{N_R} [\frac{\sqrt{2}\,\sigma_i}{S_R})^b \Gamma(\frac{b}{2} + 1)] \tag{2-14}$$

where

$$\Gamma(w) = 2 \int_o^\infty y^{(2w-1)} \exp[-y^2] \, dy \; ; \; w > 0$$

equation (2-14) was first derived by Miles (2).

If failure is defined as D = 1.0, then number of cycles to failure can be obtained from eq. (2-15).

$$N_F = \left[\frac{1}{N_R}\left(\frac{\sqrt{2}\,\sigma_i}{S_R}\right)^b \Gamma\left(\frac{b}{2}+1\right)\right]^{-1} \qquad (2\text{-}15)$$

where

S_R = Maximum peak stress in the spectrum

$\sqrt{2}\,\sigma_i$ = i^{th} Peak Stress

and σ_i = i^{th} RMS (Root Mean Square) stress

Rewriting eq. (2-15),

$$N_F = N_R\left(\frac{S_R}{\sqrt{2}\,\sigma_i}\right)^b \cdot \frac{1}{\Gamma\left(\frac{b}{2}+1\right)} \qquad (2\text{-}16)$$

It can be seen from eq. (2-16) that the curve representing the number of cycles to failure under random loading will be parallel to the constant amplitude S-N curve but offset along the abscissa by a factor of

$$\left(\frac{1}{\sqrt{2}}\right)^b \frac{1}{\Gamma\left(\frac{b}{2}+1\right)}, \text{ in terms of RMS stresses} \qquad (2\text{-}17a)$$

and

$$\frac{1}{\Gamma\left(\frac{b}{2}+1\right)}, \text{ in terms of peak stresses} \qquad (2\text{-}17b)$$

Further, derivations and applications of random load fatigue can be found in References 23 and 24.

2.2 Henry's Theory (3): Assumes a parabolic equation to describe the S-N curve above the endurance limit, S_E in the form:

$$N_i = \frac{c}{S_i - S_E} \quad ; \qquad S_E < S_i < 1.5\, S_E \tag{2-18}$$

where c is an S-N curve parameter.

2.2.1 Under Prestress Loading: After a material is subjected to one prestress, S_1 for n_1 cycles, change in the endurance limit is taken into account, hence modified S-N curve can be described as

$$N_i = \frac{c'}{S_i - S'_E} \tag{2-19}$$

where S'_E = new endurance limit after damage.

Damage after n_1 cycles is also dependent on the change in endurance limit, and is expressed as

$$d_1 = 1 - \frac{c'}{c} = \frac{S_E - S'_E}{S_E} \tag{2-20}$$

Introducing the relationship in eqs. (2-18) and (2-19), eq. (2-20) can be rewritten as

$$d_1 = \frac{\frac{n_1}{N_1}}{1 + \frac{S_E(1 - n_1/N_1)}{S_1 - S_E}} \tag{2-21}$$

Damage equivalent to d_1, is assumed to be done under a second stress, S_2 at a partial cycle ratio,

$$\frac{n_2^*}{N_2} = \frac{d_1 S_2}{d_1 S_E + S_2 - S_E} \tag{2-22}$$

remaining life therefore, is obtained from

$$n_2 = N_2\left(1 - \frac{n_2^*}{N_2}\right) \tag{2-23}$$

After i number of prestresses, damage as shown by Crichlow (4) is

$$d_i = \frac{\frac{n_i^*}{N_i} + \frac{n_i}{N_i}}{1 + \frac{S_E}{S_i - S_E}\left(1 - \frac{n_i^*}{N_i} - \frac{n_i}{N_i}\right)} \tag{2-24}$$

where $\frac{n_i^*}{N_i}$ can be obtained by redefining eq. (2-22) as

$$\frac{n_i^*}{N_i} = \frac{S_i d_{i-1}}{S_E d_{i-1} + S_i - S_E} \tag{2-25 a}$$

and

$$\frac{n_{i+1}^*}{N_{i+1}} = \frac{S_{i+1}\, d_i}{S_E d_i + S_{i+1} - S_E} \tag{2-25b}$$

Remaining life after the i^{th} prestress is then

$$n_{i+1} = N_{i+1}\left(1 - \frac{n_{i+1}^*}{N_{i+1}}\right) \tag{2-26}$$

which is obtained by solving eq. (2-24) and substituting the result obtained into eq. (2-25b).

The plot of eq. (2-24) is non-linear and the number of cuves required to define damage depends on the number of prestresses, therefore Henry's theory is stress-dependent.

The use of this theory does require knowledge of the endurance limit of the material and a non-linear S-N curve which does not hold for many materials.

2.3 Generalized Henry's Theory: The application of Henry's theory to linear log-log, S-N data was developed by Crichlow (4), by the introduction of the slope parameter, b. In this case eq. (2-18) becomes

$$N_i = \frac{c}{(S_i - S_E)^b} \quad ; \quad S_i > S_E \tag{2-27}$$

2.3.1 Under Prestress Loading: Damage after i number of prestresses can found to be

$$d_i = \frac{1 - (1 - \frac{n_i^*}{N_i} - \frac{n_i}{N_i})^{1/b}}{1 + \frac{S_E}{S_i - S_E}(1 - \frac{n_i^*}{N_i} - \frac{n_i}{N_i})^{1/b}} \tag{2-28}$$

where

$$\frac{n_i^*}{N_i} = 1 - \left[\frac{(S_i - S_E)(1 - d_{i-1})}{S_E d_{i-1} + S_i - S_E}\right]^b \tag{2-29}$$

Remaining life can similarly be obtained from eq. (2-26), for example:

If $i = 1$

then $\frac{n_1^*}{N_1} = 0$

$$d_1 = \frac{1 - (1 - \frac{n_1}{N_1})^{1/b}}{1 + \frac{S_E}{S_1 - S_E}(1 - \frac{n_1}{N_1})^{1/b}}$$

and partial cycle ratio

$$\frac{n_2^*}{N_2} = 1 - \left[\frac{(S_2 - S_E)(1 - d_1)}{S_E d_1 + S_2 - S_E}\right]^b$$

Remaining life therefore is

$$n_2 = N_2\left(1 - \frac{n_2^*}{N_2}\right)$$

2.4 Corten-Dolan Theory (5): Utilizes the concept of modified S-N (S-N') diagram to account for stress interaction of material under various loadings, eq. (2-2b) is modified to

$$\Sigma \frac{n_i}{N_i'} = 1 \qquad (2\text{-}30)$$

Assuming a linear log-log plot of the S-N' diagram, N_i' can be represented by

$$N_i' = N_R' \left(\frac{S_R}{S_i}\right)^{\delta} \qquad (2\text{-}31)$$

The S-N' diagram is obtained by adjusting eqs. (2-7) and (2-31) so that they intersect at reference point, (S_R, N_R) on the conventional S-N diagram.

Here S_R = maximum peak stress

consequently $N_R' = N_R$

2.4.1 Under block loading:

Eq. (2-6) is rewritten as

$$N_F = \frac{1}{\sum_{i=1}^{k} \frac{\alpha_i}{N_i'}} \tag{2-32}$$

and as stated earlier,

$$N_R = N_1 = N_R' = N_1'$$

With that in mind, the substitution of eq. (2-31) into eq. (2-32) yields fatigue life under block loading as

$$N_F = \frac{1}{\sum_{i=1}^{k} \frac{\alpha_i}{N_1} \left(\frac{S_1}{S_i}\right)^{\delta}} = \frac{N_1}{\sum_{i=1}^{k} \alpha_1 \left(\frac{S_1}{S_i}\right)^{\delta}} \tag{2-33}$$

The above equation is the same as Miner's eq. (2-8) if $\delta = b$, this relationship is illustrated in Fig. 7.

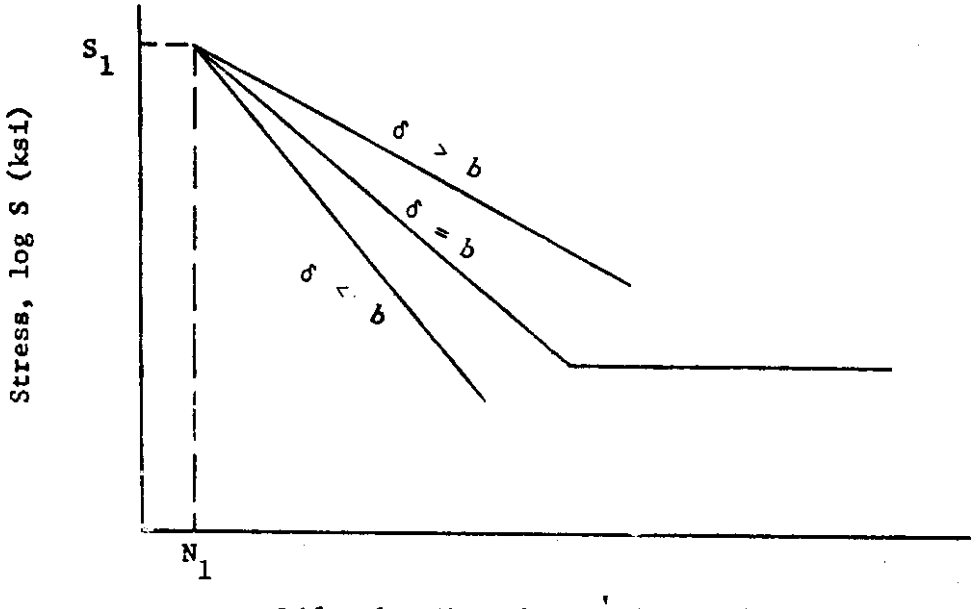

FIG. 7 LIFE DIAGRAM FOR CORTEN-DOLAN THEORY

The value of δ is determined from experiments for the different stress conditions, e.g. stress ratios. This is obtained by setting

$$R^{1/a} = \left(\frac{S_i}{S_1}\right)^{\delta}$$

and a linear regressed line or the average line representing the above equation is used to find the modified slope parameter, δ.

2.4.2 Life Prediction under Random Loading (Corten-Dolan-Rayleigh): Random fatigue life prediction using Corten-Dolan theory can be obtained by the application of eq. (2-31) to the relationship developed in eq. (2-15). In this case

$$N_F = N_R\left(\frac{S_R}{\sqrt{2}\,\sigma_i}\right)^{\delta} \frac{1}{\Gamma\left(\frac{\delta}{2} + 1\right)} \qquad (2\text{-}34)$$

2.5 Manson-Nachtigall-Freche Theory (6): Developed for fatigue damage of cyclically prestressed steel in bending. It is based on the modified S-N diagram but as opposed to Corten-Dolan theory, the point of intersection of the S-N and S-N' diagrams is assumed to lie between N = 100 cycles and N = 1000 cycles. A linear relationship is assumed between stress cycles, S and log of life N, up to the endurance limit.

The theory recognizes the change in the endurance limit after each prestress, but assumes the endurance life at the knee of the various S-N lines remains the same.

The S-N' diagram is dependent on the amount and number of prestress and on the cycle ratios.

2.5.1 Under Prestress Loading: Remaining life after $(i-1)^{th}$ prestress is given as

$$n_i = N_i \left\{ \ldots \left[\left(1 - \frac{n_1}{N_1}\right) \frac{\log N_2/N_R}{\log N_1/N_R} - \frac{n_2}{N_2} \right] \frac{\log N_3/N_R}{\log N_2/N_R} - \frac{n_i}{N_i} \right\} \frac{\log N_i/N_R}{\log N_{i-1}/N_R} \quad \text{-------} \quad (2\text{-}35)$$

This relalionship is shown in Fig. 8 for i = 2.

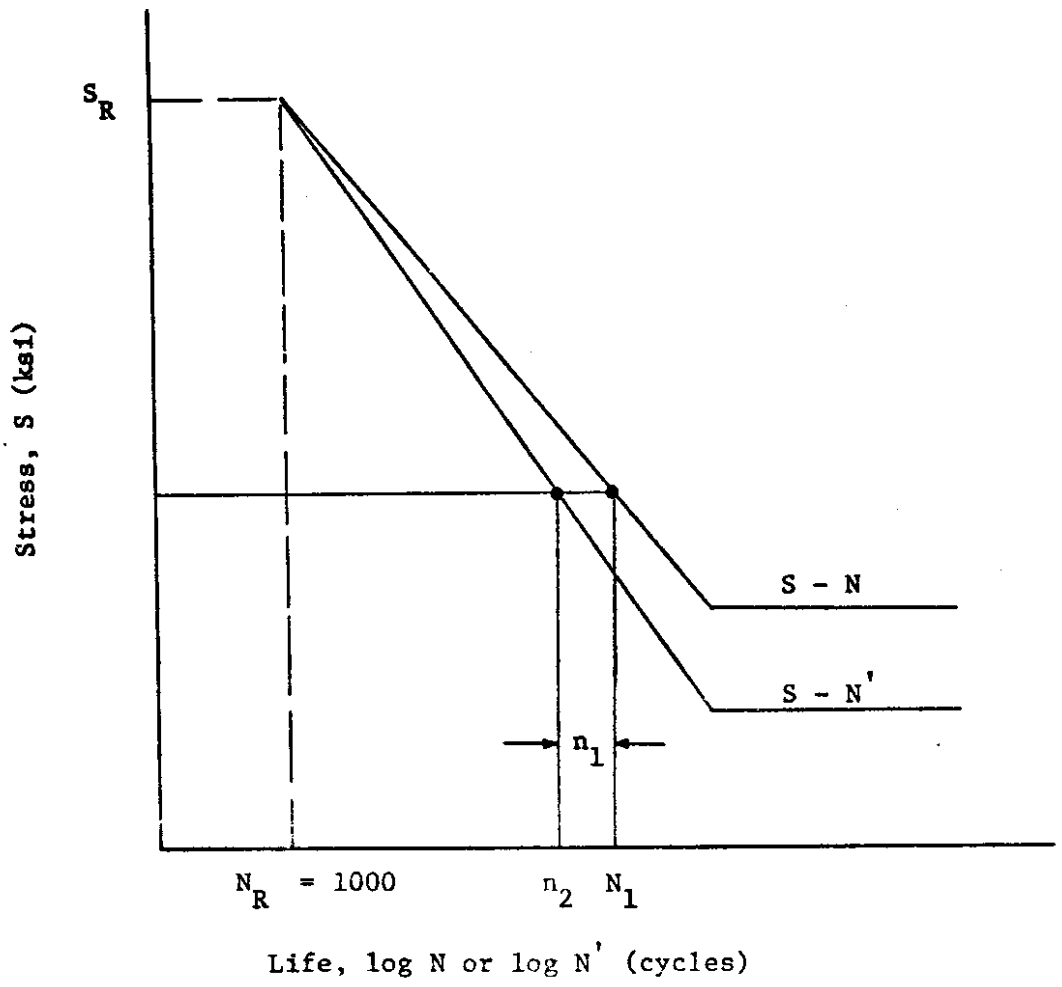

FIG. 8 LIFE DIAGRAM FOR MANSON ET AL. THEORY

2.6 Valluri's Theory: (7) Derived from the relationship between crack length and number of applied stress cycle inducing that crack. This relationship is expressed as

$$\ln \frac{L_F}{L_o} = a \frac{\left(\frac{S_i - S_{E,i}}{E}\right)^2 \left(\frac{S_i - S_{i,min}}{S_{E,i}}\right)^2}{\ln \left(\frac{S_i - S_{E,i}}{K}\right)} N_F \qquad (2\text{-}36)$$

where S_i = maximum cyclic stress applied

$S_{E,i}$ = endurance limit before i^{th} stress application

E = modulus of elasticity

K, a = material constants determined from test

N_F = number of cycles to failure

$S_{i,min}$ = minimum cyclic stress

L_F = critical crack length at N_F

L_o = Griffith's failure crack length

From Griffith's crack theory,

$$\frac{L_F}{L_o} = \left(\frac{S_u}{S_i}\right)^2 \qquad (2\text{-}37a)$$

or

$$\ln \left(\frac{L_F}{L_o}\right) = 2 \ln \left(\frac{S_u}{S_i}\right) \qquad (2\text{-}37b)$$

where S_u = ultimate tensile strength

Substituting eq. (2-37b) into eq. (2-36), number of cycles to failure is found to be

$$N_F = \frac{2}{a} \frac{\ln \left(\frac{S_u}{S_i}\right) \ln \left(\frac{S_i - S_{E,i}}{K}\right)}{\left(\frac{S_i - S_{E,i}}{E}\right)^2 \left(\frac{S_i - S_{i,min}}{S_{E,i}}\right)^2} \qquad (2\text{-}38)$$

2.6.1 Under Prestress Loading: In a two-stress step loading for example where S_1 is first applied. L_1 is crack length produced after n_1 cycles under stress S_1 thus

$$\ln\left(\frac{L_1}{Lo}\right) = \frac{\left(\frac{S_1 - S_{E1}}{E}\right)^2 \left(\frac{S_1 - S_{1min}}{S_{E1}}\right)^2}{\ln\left(\frac{S_1 - S_{E1}}{K}\right)} \quad n_1$$

An equivalent crack length ratio, $\ln\left(\frac{L_1}{Lo}\right)$ is assumed to be induced under stress, S_2 at partial cycle, n_2^* given as

$$n_2^* = n_1\left(\frac{S_1 - S_{E1}}{S_2 - S_{E2}}\right)^2 \left(\frac{S_1 - S_{1min}}{S_2 - S_{2min}}\right)^2 \left(\frac{S_{E2}}{S_{E1}}\right)^2 \frac{\ln\left(\frac{S_2 - S_{E2}}{K}\right)}{\ln\left(\frac{S_1 - S_{E1}}{K}\right)} \qquad \text{------ (2-39)}$$

The last term in eq. (2-39) is approximately unity. Remaining life therefore, at S_2 is

$$n_2 = N_2 - n_2^* = N_2 - n_1\left[\left(\frac{S_1 - S_{E1}}{S_2 - S_{E2}}\right)\left(\frac{S_1 - S_{1min}}{S_2 - S_{2min}}\right)\left(\frac{S_{E2}}{S_{E1}}\right)^2\right] \qquad \text{------ (2-40)}$$

Total damage,

$$D = \frac{n_1}{N_1} + \frac{n_2}{N_2}$$

$$= \frac{n_1}{N_1} + \frac{N_2 - n_2^*}{N_2}$$

$$= 1 + \frac{n_1}{N_1} - \frac{n_2^*}{N_2} \qquad (2\text{-}41)$$

In general, after $(i-1)^{th}$ prestresses, remaining life can be obtained from the expression

$$n_i = N_i - \sum_{j=1}^{m} n_j^* \quad ; \quad m = i \tag{2-42}$$

where

$$n_j^* = n_k \left[\left(\frac{S_k - S_{E,k}}{S_i - S_{E,i}} \right) \left(\frac{S_k - S_{k,min}}{S_i - S_{i,min}} \right) \left(\frac{S_{E,i}}{S_{E,k}} \right) \right]^2 \quad ; \tag{2-43}$$

$$(k = j - 1)$$

It should be pointed out that, for prestress conditions this method is not applicable after certain number of life has been reached. For example, after n_1, prestress cycles at S_1 stress level, crack length might have become critical that the prediction of remaining life at a different stress level, S_2 in this instance, will be unreasonable. This limiting value of critical initial prestress can be calculated from

$$(n_i)_{crit} = \frac{2}{a} \frac{\ln \left(\frac{S_u}{S_{i+1}} \right) \ln \left(\frac{S_i - S_{E,i}}{K} \right)}{\left(\frac{S_i - S_{E,i}}{E} \right)^2 \left(\frac{S_i - S_{i,min}}{S_E} \right)^2} \tag{2-44}$$

The knowledge of the material constants a, E and K are essential parameters in determining the critical prestress as indicated in eq. (2-44).

2.6.2 Under Block Loading: Under this condition, it is necessary to redefine eq. (2-42). This is accomplished by letting

m = number of stress pulses per block

and $i = 1$

Thus $N_1 = \sum_{j=1}^{m} n_j^*$

Recalling also that the cycle ratio, α_i can be expressed as either a fraction of cycles per block under i^{th} stress or as fraction of total life under i^{th} stress, hence number of cycles to failure can stated as

$$N_F = \frac{N_1}{\sum_{i=1}^{m} \alpha_i \left[\left(\frac{S_i - S_{E,i}}{S_1 - S_{E,1}}\right)\left(\frac{S_i - S_{i,min}}{S_1 - S_{1,min}}\right)\left(\frac{S_{E,1}}{S_{E,i}}\right)^2\right]} \qquad (2\text{-}45)$$

2.7 Freudenthal-Heller Theory (8): Assumes a conventional S-N and a modified S-N diagram based on random multi-stress history, as shown in Fig. 9, represented by the following equations:

$$N_i = N_R \left(\frac{S_R}{S_i}\right)^b \qquad (2\text{-}46)$$

and

$$N_i' = N_R \left(\frac{S_R}{S_i}\right)^\delta \qquad (2\text{-}47)$$

where

S_R = Reference stress corresponding to the intersection of the S-N and S-N' diagrams

N_R = Life corresponding to S_R and assumed to lie between 10^3 and 10^4 cycles.

$1/\delta$ = Slope of the S-N' diagram, varying from 4.0 to 16.0

$1/b$ = Slope of the S-N diagram

From eq. (2-6), the number of cycles to failure based on S-N' diagram is

$$N'_F = \frac{1}{\Sigma \frac{\alpha_i}{N'_i}} \quad ; \quad N'_i = \frac{N_i}{\xi_i} \tag{2-48}$$

where ξ_i = stress interaction factor ($\xi_i = 1$ for Miner) and based on S-N diagram is

$$N_F = \frac{1}{\Sigma \frac{\alpha_i}{N_i}} \tag{2-49}$$

Combining eqs. (2-48) and (2-49)

$$N'_F = \frac{N_F \Sigma \frac{\alpha_i}{N_i}}{\Sigma \frac{\alpha_i}{N'_i}} = N_F \frac{\Sigma \alpha_i (\frac{S_i}{S_R})^b}{\Sigma \alpha_i (\frac{S_i}{S_R})^\delta} \tag{2-50}$$

Total damage is obtained from

$$D = \frac{N'_F}{N_F} = \frac{\Sigma \alpha_i (\frac{S_i}{S_R})^b}{\Sigma \alpha_i (\frac{S_i}{S_R})^\delta} \tag{2-51}$$

Eq. (2-51) will give D = 1.0 as proposed by Miner's of $b = \delta$. See eq. (2-2a)

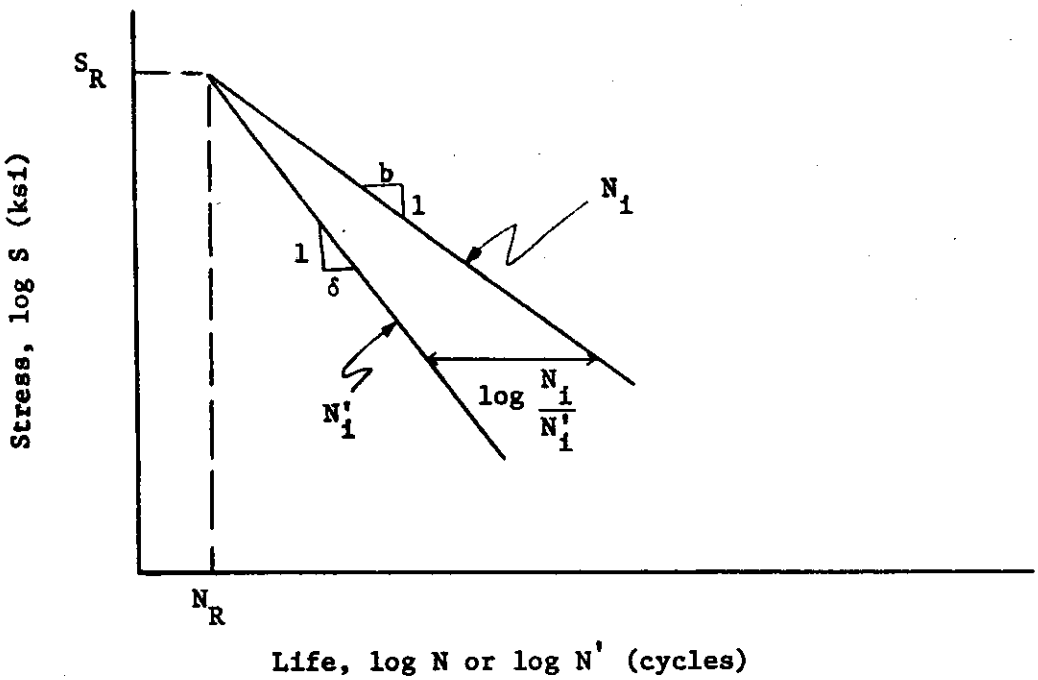

FIG. 9 LIFE DIAGRAM FOR FREUDENTHAL'S THEORY

2.7.1 Random Loading Fatigue Prediction (Freudenthal-Rayleigh):

Using the relationship obtained in eq. (2-15)

$$N_F = \left[\frac{1}{N_R}\left(\frac{\sqrt{2}\,\sigma_i}{S_R}\right)^b \Gamma\left(\frac{b}{2}+1\right)\right]^{-1}$$

and

$$N'_F = \left[\frac{1}{N_R}\left(\frac{\sqrt{2}\,\sigma_i}{S_R}\right)^\delta \Gamma\left(\frac{\delta}{2}+1\right)\right]^{-1}$$

From eq. (2-51) total damage is

$$D = \frac{N'_F}{N_F} = \left(\frac{\sqrt{2}\,\sigma_i}{S_R}\right)^{b-\delta} \frac{\Gamma\left(\frac{b}{2}+1\right)}{\Gamma\left(\frac{\delta}{2}+1\right)} \qquad (2\text{-}52a)$$

and

$$N_F' = N_F \left(\frac{\sqrt{2}\,\sigma_i}{S_R}\right)^{b-\delta} \frac{\Gamma(\frac{b}{2}+1)}{\Gamma(\frac{\delta}{2}+1)} \qquad (2\text{-}52b)$$

(S_R in terms of Peak stress)

Eq. (2-52b) will yield life prediction, $\left(\frac{\sqrt{2}\,\sigma_i}{S_R}\right)^{b-\delta} \frac{\Gamma(\frac{b}{2}+1)}{\Gamma(\frac{\delta}{2}+1)}$ times Miner's prediction, see eq. (2-16)

2.8 Grover's Theory (9): Assumes fatigue damage compose of an initial stage when cracks are nucleated by N_F'' cycles and a final stage when cracks are propagated until failure by N_F''' cycles. Thus the number of cycles to failure can be expressed as

$$N_i = N_i'' + N_i''' \qquad (2\text{-}53a)$$

or

$$1 = \frac{N_i''}{N_i} + \frac{N_i'''}{N_i} \qquad (2\text{-}53b)$$

The relationship between the above equations is shown in figure 10.

2.8.1 Under Prestress Loading: When imposed number of cycles n_1 is less than N_1'' under stress S_1 the number of cycles is failure under stress S_2 is

$$N_F = n_2 = N_2\left[1 - \frac{n_1}{N_1''} \cdot \frac{N_2''}{N_1}\right] \qquad (2\text{-}54)$$

When n_1 is greater than N_1'' under the above condition

$$N_F = n_2 = [1 - \frac{n_1}{N_1}] \frac{N_1 N_2'''}{N_1'''} \qquad (2\text{-}55)$$

It will be noticed that eq. (2-54) and eq. (2-55) will be identical to Miner's Law eq. (2-3), if the initial stage of damage as proposed in this theory is not considers i.e.

$$N_2 = N_2''$$

and

$$N_1 = N_1''$$

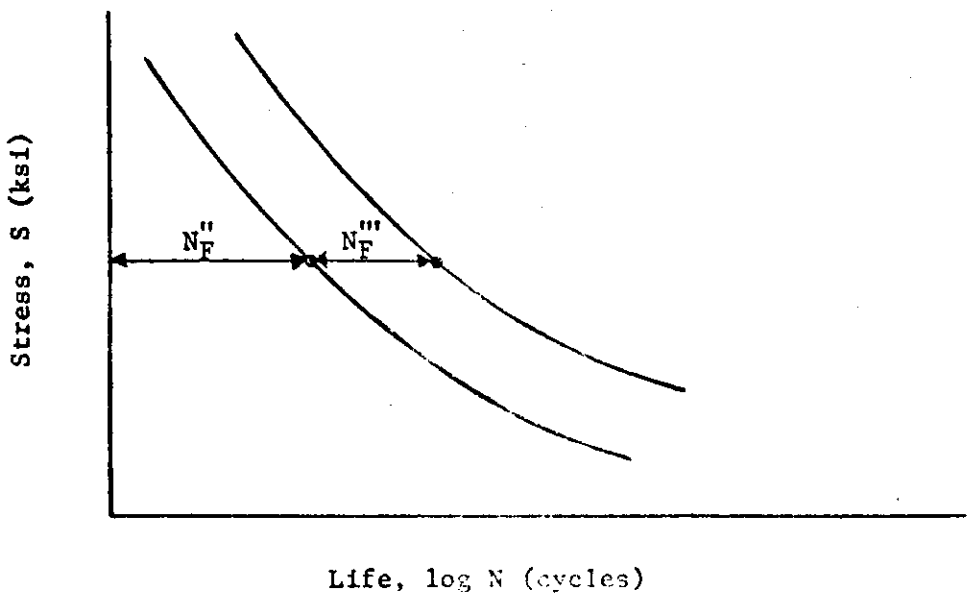

FIG. 10 SCHEMATIC REPRESENTATION OF INITIAL AND FINAL DAMAGE STAGES USING GROVER'S THEORY

2.9 Assumptions: The above eight theories are based on separate assumptions. A generally held view of the assumptions of Miner's work are:

1. The amount of damage absorbed by the material is constant under a given cyclic load-application.

2. Total damage, which constitutes failure, is the same for each specimen.

3. The amount of damage under each cyclic load is independent of the sequence of application. Hence total damage is the linear sumation of the damages absorbed during each load cycle.

However, it has been observed by many investigators (10, 11, 12, 13, 14, 15) that these assumptions are not in accord with our actual knowledge of the behavior of materials. For instance, metals are very sensitive to the order of stress applications. In spite of this, it is evident that the use of Miner's theory leads to fairly valid results. This suggests that the above assumptions are over-restrictive and that the theory is more generally applicable. From statistical arguments, Saunders (16) has widened the assumptions to the following:

1. Fatigue failure occurs when a random critical crack length is reached.

2. The incremental crack extension during a previous loading cycle is non-negative and a random variable which depends on that loading only.

3. All incremental crack extentions are non-negative, independent of one another and each independent of the critical crack length.

4. Any set of loading condition can be referred to the constant amplitude life diagram.

This consideration of assumptions can be extended to other theories. From our point of view we will tabulate such assumptions under two headings.

a. The applied loading conditions

and b. The failure conditions

Theory	Applied Loading Conditions	Failure Conditions
Miner	as stated above	as stated above
Henry	Stresses above the endurance limit introduce local stress concentration which reduces fatigue life. Damage is a function of the reduction in endurance limit.	Total damage is the sum sum of cycle ratios
Corten-Dolan	Damage depends on the formation of a number of minute cracks which propagate at all loads. The number of cracks formed is a function of the highest stress in the load spectrum.	Total damage the sum of cycle ratios.
Manson et al.	Fatigue life curves of the original and initially stressed material converge at regions of high stress due to unpronounced effects of stress concentrations.	Total damage is the sum of cycle ratios.
Valluri	Damage is a function of crack length which grows faster at higher stress levels	Failure occurs when a critical crack length is reached.
Freudenthal-Heller	Stress interaction between applied stress amplitudes depends on the probability function of the load spectrum.	Total damage is a function of the stress interaction factor
Grover	Maximum damage at the initial & final fatigue stages are constant. The ratio of the boundary between the two fatigue stages is constant.	Total damage is the sum of the damages at the initial & final stages of damage process.

3. NUMERICAL COMPARISON

3.1 The life prediction equations given in the Miner, Henry, Corten-Dolan, Manson, Valluri and Freudenthal theories are applied to some fatigue test data. Quantitative comparison is made between those theories whose parameters can be determined from test information, Grover's theory was not at all considered under those circumstances.

Tables 1 to 4 show results for four loading cases. Methods of computations and typical parametric values obtained for each theory are given in the appendix. These four cases are:

1. Prestressed material tested to failure at a singe stress level.
2. Prestressed material tested to failure over a complete range of stress levels.
3. Material tested under multi-level stress block loading.
4. Material tested under random loading.

Case 1. Prestressed Material Tested to Failure at a Single Stress Level.

Shown in table 1 are life predictions obtained from methods proposed by Miner, Henry, Manson and Valluri using eqs. (2-3), (2-23), (2-35) and (2-40).

It will be observed that all the predictions generally overestimate fatigue life. Manson's prediction, in most cases fall between Miner's and Henry's, while Valluri's prediction tend to give the highest or lowest value.

Almost in every case, Miner's prediction are less than Henry's for $\frac{S_1}{S_2} < 1.0$ and higher values for $\frac{S_1}{S_2} > 1.0$. All the theories give relatively close predictions to test results at $S_2 = 54$ ksi (which is about 86% of the yield strength). As additional testing was not done at $S_2 > 54$, a trend cannot be suggested.

Figure 11 shows the histogram of damage from test of 20 specimen, each tested at one test point. The following observations are made.

All specimens failed at	$D \geq 0.7$		
60% failed at	$D < 1.0$	(unconservative using Miner's hypothesis)	
40% failed at	$D \leq 1.0$	(conservative using Miner's hypothesis)	

TABLE 1

Data of Prestress Test of Notched SAE 4130 Steel in Bending (17)
(S_y = 62.5 ksi, S_u = 104.2 ksi, S_E = 39.0 ksi)

Stresses (ksi)		Cycle ratio	Constant Ampl. life		Remaining Life, n_2 (x 10^3 cycles)					Total Damage, D				
S_1	S_2	n_1/N_1	$N_1 \times 10^3$ (cyc.)	$N_2 \times 10^3$ (cyc.)	Test	Miner	Henry	Manson	Valluri	Test	Miner	Henry	Manson	Valluri
		0.10			198	238	253	242	256	0.850	1.00	1.059	1.018	1.070
		0.25			220	198	234	209	243	1.083	"	1.138	1.042	1.170
42	48	0.50	963	264	192	132	191	150	223	1.227	"	1.225	1.070	1.345
		0.75			177	66	123	86	202	1.420	"	1.216	1.075	1.515
		0.90			11	26	59	41	189	0.942	"	1.125	1.054	1.616
		0.10			205	238	227	232	231	0.877	"	0.958	0.978	0.975
		0.25			125	198	177	185	182	0.723	"	0.919	0.952	0.939
54	48	0.50	93	264	72	132	106	112	101	0.773	"	0.902	0.926	0.883
		0.75			50	66	48	48	18	0.939	"	0.933	0.933	0.968
		0.90			12	6	18	16	- 30*	0.945	"	0.970	0.959	
		0.10			87	84	87	85	85	1.035	"	1.032	1.018	1.014
		0.25			73	70	76	74	74	1.035	"	1.066	1.041	1.046
48	54	0.50	264	93	59	47	56	53	55	1.134	"	1.097	1.069	1.091
		0.75			27	23	31	30	37	1.040	"	1.081	1.074	1.148
		0.90			3	9	13	14	25	0.932	"	1.041	1.054	1.169
		0.10			84	84	82	82	82	1.003	"	0.979	0.981	0.982
		0.25			63	70	66	66	66	0.927	"	0.955	0.959	0.960
60	54	0.50	44	93	31	47	41	41	40	0.833	"	0.943	0.936	0.930
		0.75			15	23	19	18	13	0.911	"	0.959	0.940	0.890
		0.90			3	9	8	6	- 3*	0.932	"	0.981	0.963	

* See eq. (2-37)

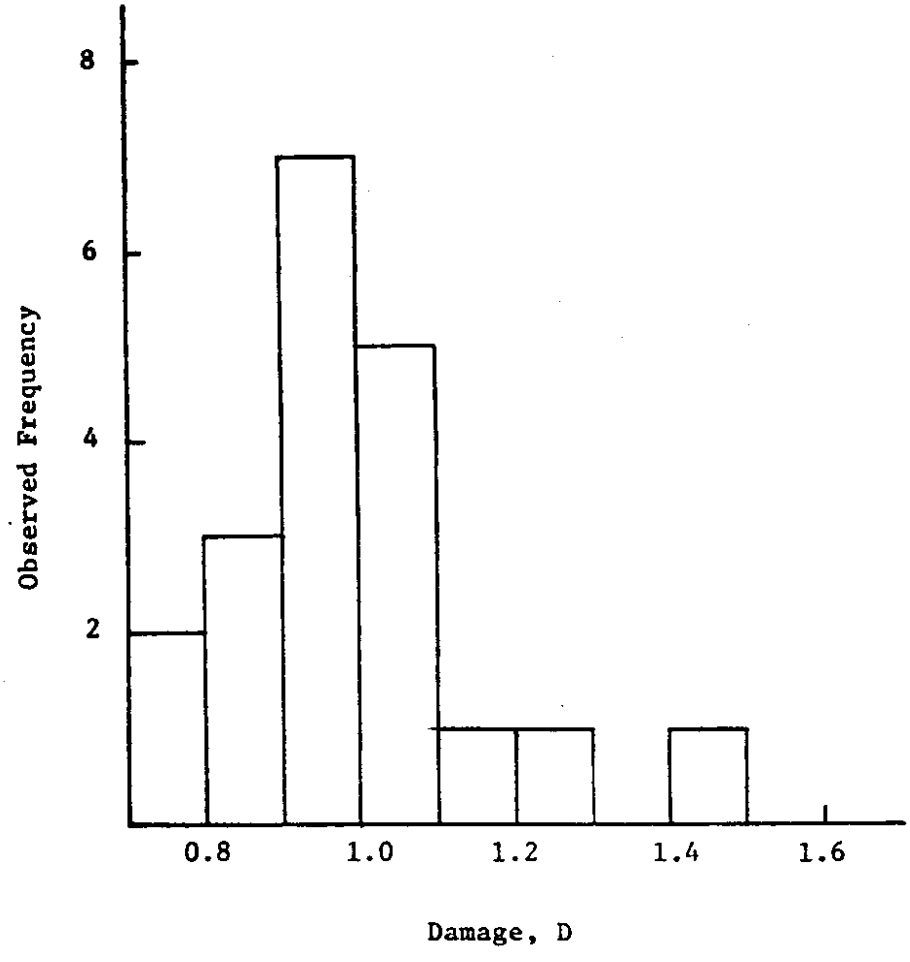

FIG. 11 HISTOGRAM OF TOTAL DAMAGE FOR 20 PRESTRESSED SPECIMENS

Case 2. Prestressed Material Tested Over a Complete Range of Stress Levels.

Table 2 shows a similar analysis to that made in Table 1. Here, it is possible to make a better comparison between the Miner, Henry, Generalized Henry, Manson and Valluri theories, over a fatigue stress range following an initial damage.

The observations made in case 1 generally hold under this condition. It should be added however, that for S_2 close to S_y and S_1 less than S_y, all the theories under consideration give mostly conservative predictions. For this set of data, Miner's theory is generally conservative when $S_1/S_2 < 1$, this may not be taken as a general trend when results of similar conditions in Table 1 are considered.

Test results given in the presented data represent mean values of ten specimen tested at each stress combination. Based on this, the damage histogram in Figure 12 shows that

All specimens failed at $D \geq 0.6$

50% failed at $D < 1.0$

50% failed at $D \geq 1.0$

Damage curves for all the prestress conditions are shown in Figs. 13a to 13d. Healing effects (negative damage) which are exhibited at low initial prestresses are not indicated by any of the damage theories, which in general give $n_2/N_2 < 1.0$.

TABLE 2

Data of Prestress Test of SAE 4340 Steel in Rotating Cantilever Beam (18)
(S_y = 145 ksi, S_u = 156 ksi, S_e = 85 ksi)

Stresses (ksi)		Cycle ratio	Constant Ampl. life		Remaining Life, n_2 (x 10^3 cycles)						Total Damage, D					
S_1	S_2	n_1/N_1	$N_1 \times 10^3$ (cyc.)	$N_2 \times 10^3$ (cyc.)	Test	Miner	Henry	Gen. Henry*	Manson	Valluri	Test	Miner	Henry	Gen. Henry	Manson	Valluri
95.9	106.6	0.05	234.5	83.8	89.5	79.6	81.4	81.4	80.4	81.4	1.118	1.00	1.021	1.021	1.009	1.021
		0.15			81.3	71.2	76.4	76.5	73.4	76.6	1.120	"	1.061	1.063	1.026	1.064
		0.35			76.4	54.5	64.6	65.6	59.1	66.9	1.262	"	1.121	1.133	1.055	1.148
		0.70			50.9	25.1	36.5	41.8	31.5	50.0	1.308	"	1.135	1.199	1.076	1.297
	117.3	0.05		37.1	39.6	35.3	36.3	36.3	35.9	36.2	1.117	"	1.028	1.028	1.017	1.026
		0.15			42.0	31.5	34.7	36.7	33.3	34.4	1.282	"	1.084	1.139	1.048	1.077
		0.35			27.5	24.1	30.5	36.4	27.9	30.9	1.091	"	1.171	1.331	1.102	1.183
		0.70			21.1	11.2	19.0	22.1	16.7	24.6	1.269	"	1.212	1.296	1.151	1.363
	127.9	0.05		14.75	15.8	14.0	14.5	14.5	14.4	14.3	1.121	"	1.032	1.033	1.025	1.019
		0.15			16.1	12.3	13.9	14.0	13.6	13.5	1.242	"	1.095	1.099	1.073	1.065
		0.35			14.0	9.6	12.5	12.7	11.9	11.8	1.299	"	1.199	1.211	1.159	1.150
		0.70			10.8	4.6	8.3	9.6	8.1	8.8	1.432	"	1.262	1.351	1.252	1.297
106.6	95.9	0.05	83.8	234.5	190.5	222.8	215.0	214.1	220.2	214.2	0.862	"	0.967	0.963	0.989	0.963
		0.15			147.9	199.3	178.0	175.9	191.8	173.5	0.781	"	0.909	0.900	0.968	0.890
		0.35			121.9	152.4	119.1	110.3	137.9	92.2	0.870	"	0.858	0.820	0.938	0.744
		0.70			55.5	70.4	45.0	30.3	53.2	**	0.937	"	0.892	0.829	0.927	
	117.3	0.05		37.1	35.2	35.3	35.8	35.7	35.6	35.6	0.999	"	1.014	1.012	1.009	1.010
		0.15			38.2	31.5	31.8	32.9	32.5	32.5	1.180	"	1.006	1.037	1.026	1.026
		0.35			30.9	24.1	26.6	27.0	26.1	26.3	1.183	"	1.067	1.078	1.054	1.059
		0.70			17.3	11.1	13.7	15.1	13.9	15.4	1.166	"	1.069	1.107	1.074	1.115
	127.9	0.05		14.75	14.9	14.0	14.3	14.3	14.3	14.0	1.060	"	1.021	1.019	1.019	1.000
		0.15			15.8	12.5	13.3	13.4	13.4	12.5	1.221	"	1.034	1.058	1.056	"
		0.35			14.0	9.6	11.2	11.3	11.4	9.6	1.299	"	1.106	1.116	1.120	"
		0.70			5.9	4.4	6.8	7.0	7.1	4.4	1.100	"	1.162	1.175	1.181	"
117.3	95.9	0.05	37.1	234.5	161.1	222.8	208.0	207.2	216.9	210.1	0.737	"	0.937	0.934	0.975	0.946
		0.15			127.3	199.3	163.4	158.9	184.6	161.4	0.693	"	0.847	0.828	0.927	0.838
		0.35			81.3	152.4	101.1	85.3	122.4	63.9	0.697	"	0.781	0.714	0.872	0.622
		0.70			25.7	70.4	34.9	16.0	38.0	***	0.810	"	0.849	0.768	0.862	
	106.6	0.05		83.8	77.3	79.6	78.3	78.2	98.7	78.8	0.972	"	0.984	0.983	0.989	0.990
		0.15			77.5	71.2	67.5	67.2	68.6	68.7	1.074	"	0.956	0.952	0.969	0.970
		0.35			45.0	54.5	48.4	46.9	49.4	48.6	0.887	"	0.927	0.910	0.940	0.930
		0.70			22.1	25.1	20.0	17.0	19.2	13.5	0.964	"	0.939	0.903	0.929	0.861
	127.9	0.05		14.75	15.0	14.0	14.2	14.1	14.2	13.9	1.067	"	1.009	1.006	1.013	0.992
		0.15			13.0	12.5	12.9	12.9	13.1	12.1	1.031	"	1.024	1.023	1.036	0.970
		0.35			11.1	9.6	10.2	10.3	10.7	8.6	1.103	"	1.044	1.048	1.076	0.933
		0.70			6.5	4.4	5.1	5.4	6.0	2.4	1.141	"	1.044	1.066	1.108	0.863
127.9	95.9	0.05	14.75	234.5	135.8	222.8	202.8	201.7	211.3	214.2	0.629	"	0.915	0.910	0.951	0.953
		0.15			112.2	199.3	152.9	146.3	168.6	173.5	0.628	"	0.802	0.774	0.869	0.890
		0.35			60.0	152.4	83.8	69.4	97.8	92.3	0.606	"	0.733	0.646	0.767	0.744
		0.70			28.3	70.4	29.3	9.8	20.4	**	0.821	"	0.825	0.742	0.787	
	106.6	0.05		83.8	76.2	79.6	77.1	77.0	77.0	79.6	0.959	"	0.970	0.969	0.969	1.000
		0.15			51.6	71.2	64.6	64.1	64.1	71.2	0.766	"	0.921	0.915	0.915	"
		0.35			36.5	54.5	44.2	41.5	41.2	54.5	0.786	"	0.877	0.845	0.842	"
		0.70			13.4	25.1	17.1	12.3	11.6	25.2	0.860	"	0.904	0.847	0.838	"
	117.3	0.05		37.1	33.1	35.3	34.9	34.9	34.6	35.6	0.942	"	0.990	0.991	0.983	1.010
		0.15			26.1	31.5	30.5	30.4	29.8	32.5	0.854	"	0.971	0.969	0.954	1.026
		0.35			16.9	24.1	22.6	22.0	20.8	25.3	0.786	"	0.958	0.943	0.911	1.059
		0.70			10.5	11.1	9.6	8.7	7.4	15.4	0.983	"	0.959	0.935	0.899	1.115

* Taking b = 9.2
** See eq.(2-37)

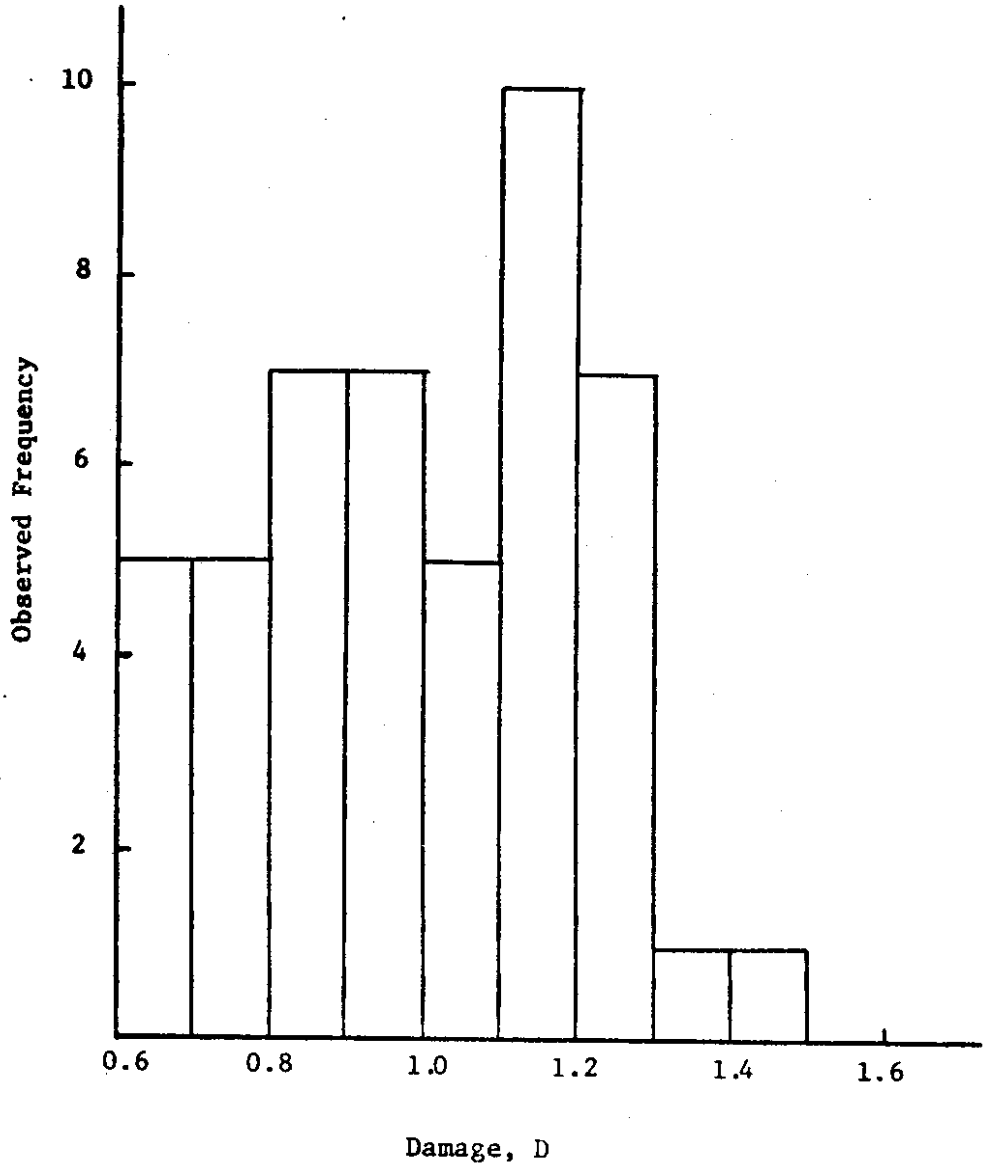

FIG. 12 HISTOGRAM OF MEAN DAMAGE FOR 48 SETS OF PRESTRESSED SPECIMENS

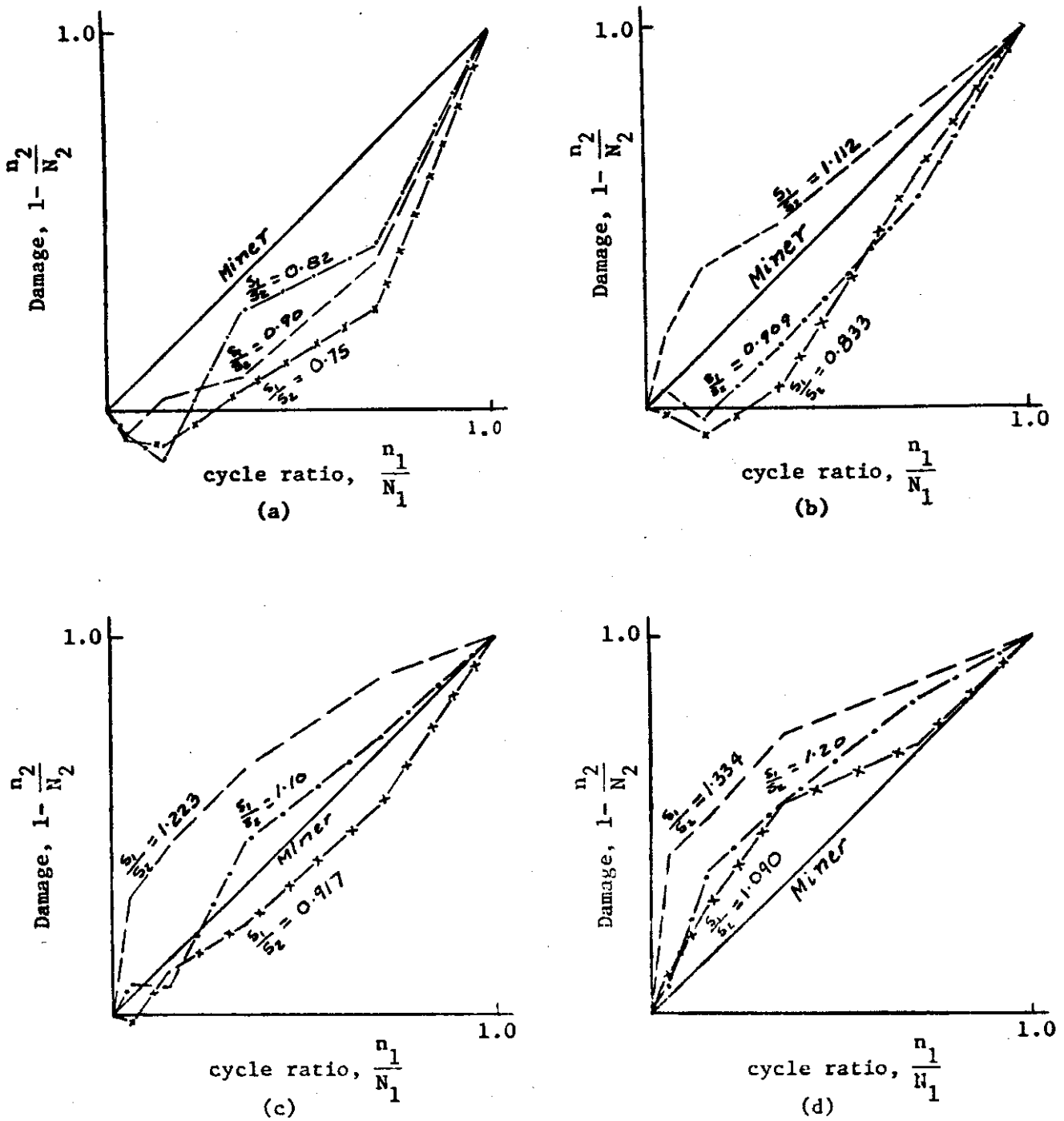

FIG. 13 DAMAGE PLOTS - (a) S_1 = 95900 psi, (b) S_1 = 106600 psi (c) S_1 = 117300 psi AND (d) S_1 = 127900 psi.

Case 3. Material Tested Under Multi-Level Stress Block Loading.

Life prediction using Miner, Corten-Dolan and Valluri methods for two-stress block loading is shown in Table 3. In this case eqs. (2-8), (2-33) and (2-45) were used.

In most cases Miner's theory gives more conservative life prediction than the other two. No particular trend can be observed between the proposed theories and the test life, nonetheless all the predictions give good agreement with the observed life.

The observed life in Table 3 is based on the mean value of between 15 and 20 specimen, hence total damage are mean values. Damage histogram shown in Fig. 14 indicates:

All specimens failed at	$D \geq 0.9$	
8.7% failed at	$D < 1.0$	
91.3% failed at	$D \geq 1.0$	

For this particular case, Miner's theory is very convervative in predicting over 90% safe life while Corten-Dolan predicts 65% and Valluri, under 20%. It has been observed in tests conducted by Schijve(34) that less scatter is experienced in fatigue life under block loading than in prestress loading, consequently D is generally greater than 1.0.

TABLE 3

Data of Two-Stress Block loading Test on 7075-T6 Aluminum Alloy in Rotating Bending (19)
(S_y = 69 ksi, S_u = 80 ksi, S_E = 20 ksi)

Stresses (ksi)		Cycle ratio	Remaining Life, n_2 (cycles)				
S_1	S_2	α_1(%)	Test(mean)	Valluri	Corten	Miner	Total Damage
50	45	9.95	30550	30970	31900	31420	0.97
50	45	3.97	33600	32370	33460	32900	1.02
50	45	0.95	31220	33120	34300	33700	0.93
50	40	9.95	48600	52780	54200	46790	1.04
50	40	3.97	60580	60000	61960	51940	1.17
50	40	0.95	62320	64450	66800	54990	1.13
50	40	0.37	61206	65380	67810	55620	1.10
50	35	9.95	87600	89460	88000	75920	1.15
50	35	3.97	118100	119300	116600	95150	1.24
50	35	0.95	132200	143500	139400	109100	1.21
50	30	9.95	135600	138500	128500	114900	1.18
50	30	3.97	248400	240300	210100	174200	1.43
50	30	0.95	350300	382100	309300	235500	1.49
50	30	0.37	363300	431000	340100	252600	1.44
50	25	9.95	163700	177500	162300	150560	1.09
50	25	3.97	362000	404800	329700	282100	1.28
50	25	0.95	1045000	1146000	688100	504800	2.07
50	20	9.95	180600	188640	180600	177500	1.02
50	20	3.97	423000	472800	422500	405000	1.04
50	20	0.95	1494000	1976000	1306000	1147000	1.30
50	35	9.85	91000	89840	88370	76170	1.19
50	35	3.81	125000	120400	117600	95800	1.30
50	35	0.87	142000	144200	140100	109500	1.29

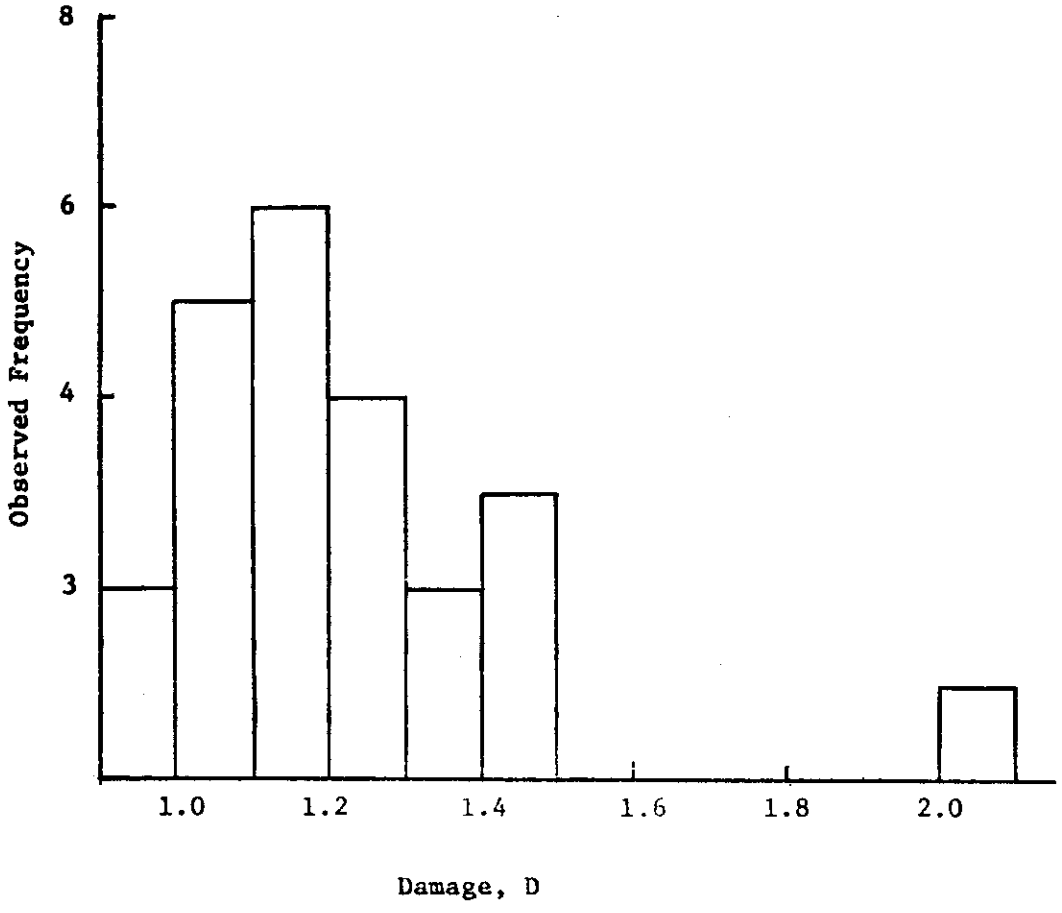

FIG. 14 HISTOGRAM OF MEAN DAMAGE FOR TWO-STRESS BLOCK LOADING OF 23 SETS OF SPECIMENS

Case 4. Material Tested Under Random Loading.

Life prediction on axially loaded aluminum specimen using Miner, Dolan-Corten and Frendenthal theories are shown in Table 4.

The constant amplitude (S-N) diagram has to be determined in terms of peak stresses as

$$N_i = \left(\frac{264}{\sqrt{2}\,\sigma_i}\right)^{5.54}$$

from which the life predictions can be determined for each theory knowing the modified slope parameter contained in the Corten-Dolan and Freudenthal's theory, (see eqs.(2-15), (2-34) and (2-52b)) given as δ=5.67 (21) and δ= 4.0(22) respectively. The resulting calculations are presented in the Appendix.

In all cases cited in Table 4, Miner's and Corten-Dolan predictions overestimated random fatigue life by at least over four and eight times respectively. Freudenthal's method predicted relatively lower life and safe life in only one instance.

Random fatigue tests by Head and Hooke (25) show Miner's hypothesis to overestimate by factors between two and three and one half, while March et al (26) and White et al (27) reported reasonable agreement between test data and Miner's predictions especially at high stresses. On the contrary, the use of Miner's theory at very low stresses (long life ranges) will yield inaccurate prediction since no damage is assumed done in that region (20, 28). Tests conducted on aluminum alloys by Hillberry (29) and Sherman (30) confirm this shortcoming.

TABLE 4

Data of Axial Random Test on 2024-T4 Aluminum Alloy (20)

Stresses (ksi)		Const. Ampl. life	Predicted Life, N_F (x 10^4 cycles)						
RMS	Peak	N_ix10^4 (cyc.)	(max)	Test (mean)	(min)	Miner	Freudenthal	Corten	Deg. of freedom
12.7	18.0	289.4	8.7	6.1	4.1	63.7	17.1	74.4	1
12.0	17.0	379.2	17.5	12.1	7.8	87.4	21.5	102.9	
11.3	16.0	555.7	38.3	28.0	17.4	122.3	27.3	145.1	
9.5	13.5	1424.4	52.5	45.2	38.6	313.4	54.7	380.3	
8.13	11.5	3462.7	117.5	69.2	42.5	761.8	101.9	943.9	
6.7	9.5	9979.2	141.4	96.5	70.2	2195.4	220.9	2788.6	
6.35	9.0	13464.3	379.7	250.4	157.0	2962.1	273.8	3790.0	
10.4	12.0	274.5		7.1		601.8	38.1	741.5	2
8.83	10.1	7108.0		23.2		1563.8	73.2	1970.5	
7.92	9.1	12664.7		60.0		2786.2	113.1	3558.9	

3.1.1 Discussion: It is evident from test results on damage accumulation that total damage is not constant for all materials as proposed by Miner nor do any of the proposed theories give results consistently close to test results. Test data do not indicate a particular trend that will allow accurate prediction of total damage, which most studies have shown to vary upwards of 0.1 and more concentrated within 0.3 and 3.0 range. It is desirable therefore, to explore a most likely lower bound value for design purposes.

Data from 815 individually tested specimens of steel and aluminum alloy were collected (this will be referred to as "individual data"). This data include test results of random, prestress, continuously varying stress and block loadings at various mean stresses with specimen loaded in bending or axially. The mean value of total damage was 1.2050 and the standard deviation 1.1915.

For purposes of comparison, similar test data on 369 groups of specimens were gathered (this will be referred to as "mean data"). In this case, each group consists of between 2 and 20 specimens, which are tested under identical stress conditions and the mean value of total damage obtained from each group represented a data point. The mean of this set of data was found to be 1.2058 and the standard deviation 1.2050.

It should be pointed out that the values and closeness of the mean damage obtained from the above two sets of data are characteristics of the data rather than representative values. The histogram for the above data, obtained from References (10,14,17,18,19,29,30,31,32,35,36 and 37) are shown in Figs. 15 and 16.

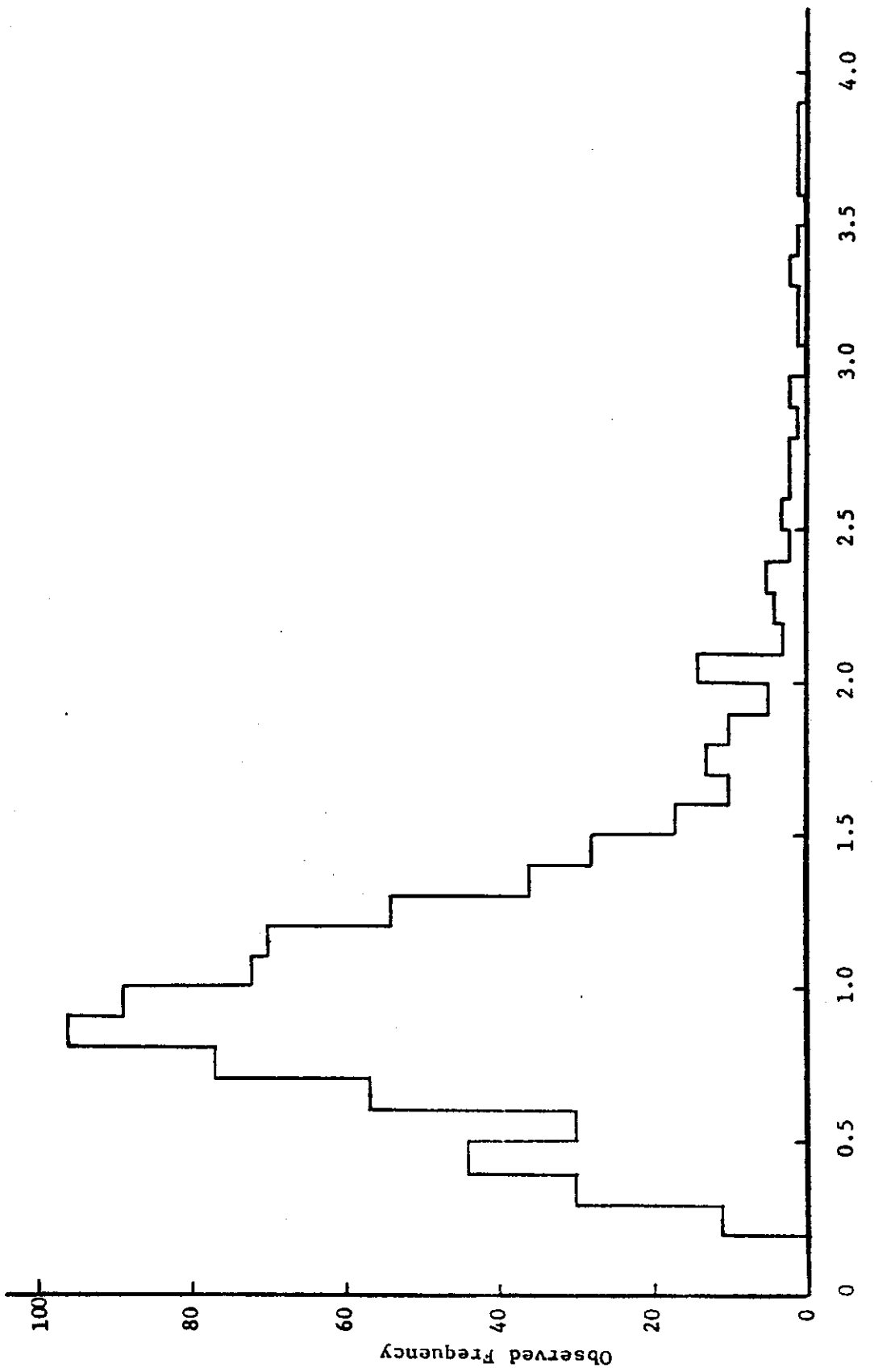

FIG. 15 HISTOGRAM OF TOTAL DAMAGE FOR 815 SPECIMENS

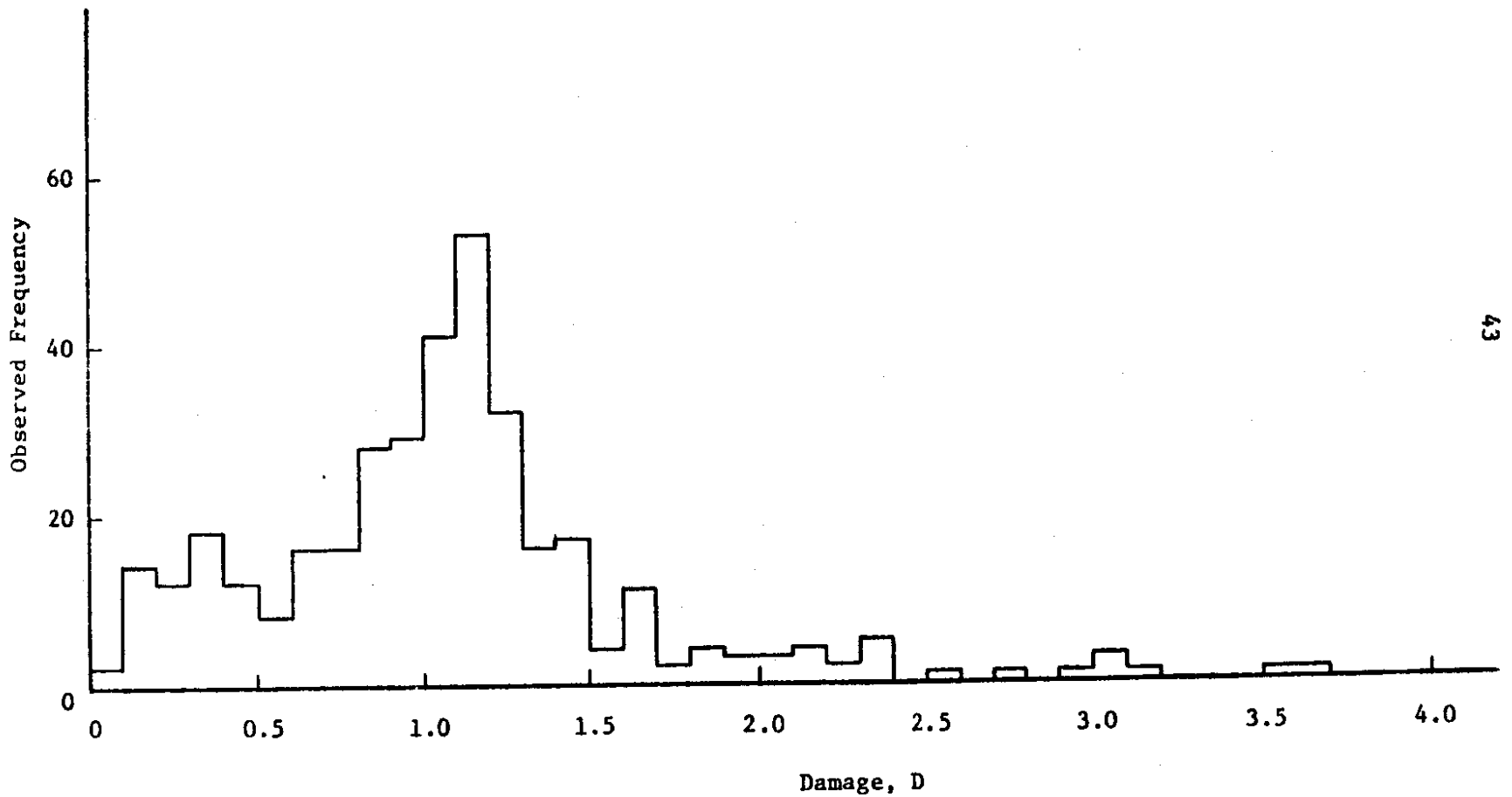

FIG. 16 HISTOGRAM OF MEAN DAMAGE FOR 369 GROUPS OF SPECIMENS

4. DAMAGE DISTRIBUTION BY MAXIMUM ENTROPY PRINCIPLES

In this section, data for fatigue damage are used to obtain probability distributions of the damage, $D = \sum_i \frac{n_i}{N_i}$. This is accomplished by using Jaynes (41) method of maximum entropy. This way, the consequent distribution is obtained with the least bias and is presented in the form of the program:

$$\text{maximize,} \qquad H = -\sum_j P_j \ln P_j \tag{4-56}$$

$$\text{subject to} \qquad \sum_j P_j = 1 \tag{4-57}$$

$$\text{and} \qquad \sum_j P_j g_k(D_j) = E_j \,, \; k = 1, 2, \ldots, r \tag{4-58}$$

where

H = entropy or uncertainty

P = probability distribution of z variables

E_k = expected value of the function $g_k(D_j)$

The unknown of this program is the probability of damage, P_j which can be written in form

$$P_j = P(D_j) = \exp\left[-\lambda_o - \sum_k \lambda_k g_k(D_j)\right] \tag{4-59}$$

where

λ_o, λ_k are Lagrangian multipliers

The Lagrangian multipliers, as shown by Tribus (42) must satisfy the constraints

$$\lambda_o = \ln \sum_j \exp \left[-\sum_k \lambda_k g_k(D_j)\right] \tag{4-60a}$$

$$\frac{\partial \lambda o}{\partial \lambda_k} = E_j \tag{4-60b}$$

$$\frac{\partial^2 \lambda o}{\partial \lambda_k^2} = s^2(g_k) \tag{4-60c}$$

For k = 2 in the restraint equation (4-58), the probability of damage in eq. (4-59) becomes

$$P(D_j) = \exp\left[-\lambda_o - \lambda_1 g_1(D_j) - \lambda_2 g_2(D_j)\right]$$

The fatigue damage data being used here, made possible the determination of the following knowledge parameters:

(a) Mean, M

(b) Variance, V

(c) Standard deviation, s

and (d) $\ln D_j$ (total damage being non-negative)

necessary to determine the distribution of damage. With the above parameters, the truncated Normal distribution and the functional Gamma distribution are utilized in the evaluation of the two sets of data (individual and mean data as described in Section 3.1.1) under consideration.

4.1 Truncated Normal Distribution (using discrete data):

Consider the constraint equations

$$\sum_{j=o}^{\infty} P_j = 1$$

$$\sum_{j=o}^{\infty} P_j D_j = M$$

$$\sum_{j=o}^{\infty} P_j D_j^2 = V$$

and the probability distribution

$$P(\bar{D}_j) = \exp[-\lambda_o - \lambda_1 \bar{D}_j - \lambda_2 \bar{D}_j^2] \qquad (4\text{-}61)$$

where $\bar{D}_j$ is the average damage value in j^{th} interval.

In order to treat this discrete data as continuous small intervals are required, a value of $D = 0.1$ seem reasonable for our purpose, as a consequence, eqs. (4-60a to c) become

$$\lambda_o = \left\{ \ln \frac{1}{\Delta D} \int_o^{\infty} \exp [-\lambda_1 D - \lambda_2 D^2] d D \right\} \qquad (4\text{-}62)$$

The solution, and derivatives of the above equation is shown by Tribus (42) as

$$\lambda_o = \frac{\lambda_1^2}{4\lambda_2} - \frac{1}{2} \ln \lambda_2 + \ln[i - \operatorname{erf} (\frac{\lambda_1}{2\sqrt{\lambda_2}})] + \ln \frac{\sqrt{\pi}}{2 \Delta D}$$

$$\frac{\partial \lambda_o}{\partial \lambda_1} = -M = \frac{\lambda_1}{2\lambda_2} - \frac{1}{\sqrt{\pi \lambda_2}} \cdot \frac{\exp (-\lambda_1^2/4\lambda_2)}{1 - \operatorname{erf}(\frac{\lambda_1}{2\sqrt{\lambda_2}})}$$

and

$$\frac{\partial \lambda_o}{\partial \lambda_2} = -M^2 - s^2 = -\frac{1}{2\lambda_2} - \frac{\lambda_1^2}{4\lambda_2^2} + \frac{\lambda_1}{2\lambda_2\sqrt{\pi\lambda_2}} \cdot \frac{\exp(-\lambda_1^2/4\lambda_2)}{1 - \text{erf}(\frac{\lambda_1}{2\sqrt{\lambda_2}})}$$

where $\text{erf}(x) = \frac{2}{\sqrt{\pi}} \int_o^x e^{-t^2} dt$

from which the Lagrangian parameters were obtained on the computer and are given below:

For the individual data, ($\Sigma x_i = 815$)

$M = 1.2050$
$s = 1.1915$
$\lambda_o = 3.19242$
$\lambda_1 = 0.791173$
$\lambda_2 = 0.008120$

For the mean data, ($\Sigma x_i = 369$)

$M = 1.2058$
$s = 1.2050$
$\lambda_o = 3.19273$
$\lambda_1 = 0.791633$
$\lambda_2 = 0.007820$

The probability distribution P_j for the above two cases are tabulated in Tables 5 and 6, also shown in Figs. 17 and 18. As can be expected, since the mean and standard deviation in both cases are almost

TABLE 5

Distribution of Damage Using Individual Test Data

			Test Distribution		Functional Gamma Distribution		Normal Distribution	
Range of D	$\bar{D}$	X_i	frequency	1-cum.freq	$P(\bar{D})$	$R(\bar{D})$	$P(\bar{D})$	$R(\bar{D})$
0.0-0.1	0.05	0	0.0	1.0	0.0002	0.9998	0.0395	0.9605
0.1-0.2	0.15	0	0.0	1.0	0.0037	0.9961	0.0365	0.9241
0.2-0.3	0.25	11	0.0135	0.9865	0.0129	0.9832	0.0337	0.8904
0.3-0.4	0.35	30	0.0368	0.9497	0.0261	0.4571	0.0311	0.8593
0.4-0.5	0.45	44	0.0540	0.8957	0.0405	0.9166	0.0287	0.8305
0.5-0.6	0.55	30	0.0368	0.8589	0.0536	0.8630	0.0265	0.8040
0.6-0.7	0.65	57	0.0699	0.7890	0.0641	0.7989	0.0245	0.7795
0.7-0.8	0.75	77	0.0945	0.6945	0.0710	0.7279	0.0226	0.7570
0.8-0.9	0.85	96	0.1178	0.5767	0.0745	0.6534	0.0208	0.7361
0.9-1.0	0.95	89	0.1092	0.4675	0.0749	0.5785	0.0192	0.7169
1.0-1.1	1.05	72	0.0883	0.3792	0.0726	0.5059	0.0177	0.6992
1.1-1.2	1.15	70	0.0859	0.2933	0.0685	0.4374	0.0164	0.6828
1.2-1.3	1.25	54	0.0663	0.2270	0.0631	0.3742	0.0151	0.6677
1.3-1.4	1.35	36	0.0442	0.1828	0.0570	0.3172	0.0139	0.6538
1.4-1.5	1.45	28	0.0344	0.1484	0.0507	0.2665	0.0128	0.6410
1.5-1.6	1.55	17	0.0209	0.1275	0.0443	0.2222	0.0118	0.6292
1.6-1.7	1.65	10	0.0123	0.1152	0.0383	0.1839	0.0109	0.6183
1.7-1.8	1.75	13	0.0160	0.0992	0.0327	0.1512	0.0100	0.6082
1.8-1.9	1.85	10	0.0123	0.0869	0.0276	0.1236	0.0092	0.5990
1.9-2.0	1.95	5	0.0061	0.0808	0.0232	0.1004	0.0085	0.5905
2.0-2.1	2.05	14	0.0172	0.0636	0.0192	0.0812	0.0078	0.5826
2.1-2.2	2.15	3	0.0037	0.0599	0.0159	0.0653	0.0072	0.5754
2.2-2.3	2.25	4	0.0049	0.0550	0.0130	0.0523	0.0066	0.5688
2.3-2.4	2.35	5	0.0061	0.0489	0.0106	0.0417	0.0061	0.5627
2.4-2.5	2.45	2	0.0025	0.0464	0.0086	0.0331	0.0056	0.5570
2.5-2.6	2.55	3	0.0037	0.0427	0.0069	0.0262	0.0052	0.5518
2.6-2.7	2.65	2	0.0025	0.0402	0.0055	0.0207	0.0048	0.5471
2.7-2.8	2.75	2	0.0025	0.0377	0.0044	0.0163	0.0044	0.5427
2.8-2.9	2.85	1	0.0012	0.0365	0.0035	0.0127	0.0040	0.5387
2.9-3.0	2.95	2	0.0025	0.0340	0.0027	0.0100	0.0037	0.5350
3.0-3.1	3.05	0	0.0	0.0340	0.0022	0.0078	0.0034	0.5315
3.1-3.2	3.15	1	0.0012	0.0328	0.0017	0.0060	0.0031	0.5284
3.2-3.3	3.25	1	0.0012	0.0316	0.0014	0.0047	0.0029	0.5255
3.3-3.4	3.35	2	0.0025	0.0291	0.0011	0.0036	0.0026	0.5229
3.4-3.5	3.45	1	0.0012	0.0279	0.0008	0.0028	0.0024	0.5204
3.5-3.6	3.55	0	0.0	0.0279	0.0006	0.0022	0.0022	0.5182
3.6-3.7	3.65	1	0.0012	0.0267	0.0005	0.0017	0.0021	0.5162
3.7-3.8	3.75	1	0.0012	0.0255	0.0004	0.0013	0.0019	0.5143
3.8-3.9	3.85	1	0.0012	0.0243	0.0003	0.0010	0.0017	0.5125
3.9-4.0	3.95	0	0.0	0.0243	0.0002	0.0008	0.0016	0.5095
4.7-4.8	4.75	1	0.0012	0.0231	0.0000	0.0001		
4.8-4.9	4.85	1	0.0012	0.0219	0.0000	0.0001		
5.1-5.2	5.15	1	0.0012	0.0207	0.0000	0.0000		
5.4-5.5	5.45	1	0.0012	0.0195	0.0000	0.0000		
5.6-5.7	5.65	2	0.0025	0.0170	0.0000	0.0000		
5.8-5.9	5.85	1	0.0012	0.0158	0.0000	0.0000		
6.1-6.2	6.15	1	0.0012	0.0146	0.0000	0.0000		
7.3-7.4	7.35	1	0.0012	0.0134	0.0000	0.0000		
7.6-7.7	7.65	1	0.0012	0.0122	0.0000	0.0000		
7.7-7.8	7.75	1	0.0012	0.0110	0.0000	0.0000		
7.9-8.0	7.95	1	0.0012	0.0098	0.0000	0.0000		
8.1-8.2	8.15	1	0.0012	0.0086	0.0000	0.0000		
8.3-8.4	8.35	1	0.0012	0.0074	0.0000	0.0000		
8.4-8.5	8.45	1	0.0012	0.0062	0.0000	0.0000		
9.3-9.4	9.35	1	0.0012	0.0050	0.0000	0.0000		
10.0-10.1	10.05	1	0.0012	0.0038	0.0000	0.0000		
10.7-10.8	10.75	1	0.0012	0.0026	0.0000	0.0000		
11.4-11.5	10.45	1	0.0012	0.0014	0.0000	0.0000		
11.9-12.0	11.95	1	0.0012	0.0002	0.0000	0.0000		

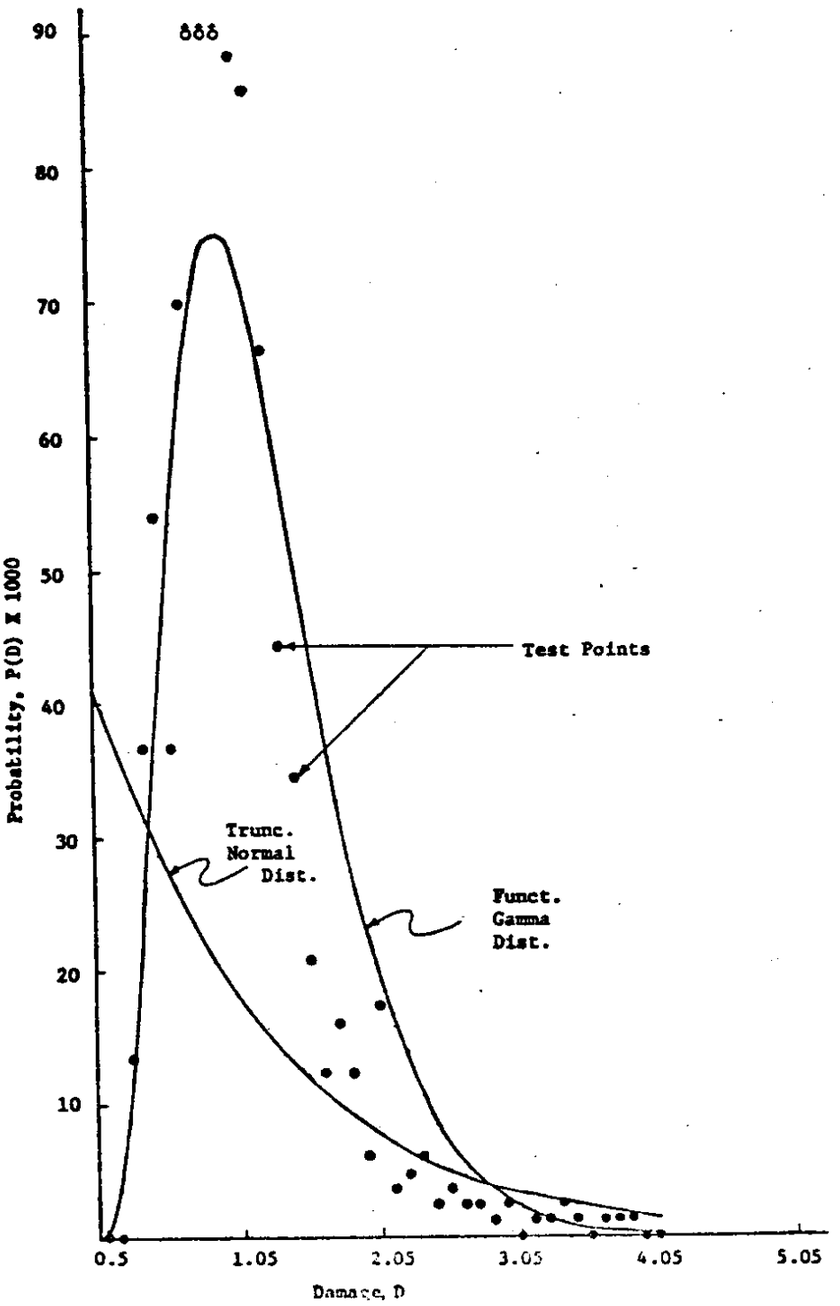

FIG. 17 DAMAGE PROBABILITY CURVES OF 815 SPECIMENS

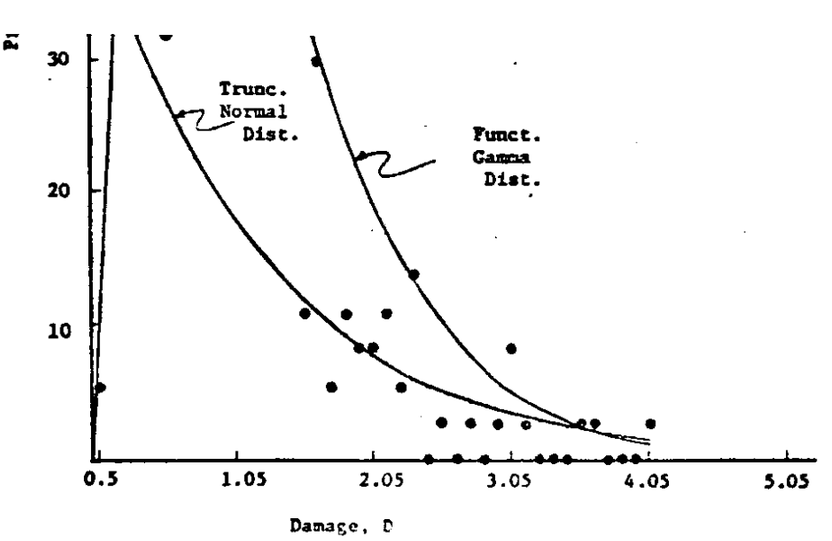

identical, the distributions approach exponential distributions.

4.2 Functional Gamma Distribution (using discrete data):

Consider the constraints

$$\sum_{j=o}^{\infty} P_j = 1$$

$$\sum_{j=o}^{\infty} P_j D_j = M$$

$$\sum_{j=o}^{\infty} P_j \ln D_j = \overline{\ln t}$$

and the probability distribution

$$P(\bar{D}_j) = \exp[-\lambda_o - \lambda_1 \bar{D}_j - \lambda_2 \ln \bar{D}_j] \qquad (4\text{-}63)$$

For small ΔD as stated earlier, eq. (4-60 a to c) become

$$\lambda_o = \ln\left\{\frac{1}{\Delta D} \int_o^{\infty} [D_j^{-\lambda_2} \cdot \exp(-\lambda_1 D_j)]\, dD\right\}$$

$$= (\lambda_2 - 1) \ln \lambda_1 + \ln \Gamma(1 - \lambda_2) - \ln \Delta D$$

and

$$\frac{\partial \lambda_o}{\partial \lambda_1} = -M = \frac{\lambda_2 - 1}{\lambda_1}$$

$$\frac{\partial \lambda_o}{\partial \lambda_2} = -\overline{\ln t} = \ln \lambda_1 + \frac{\partial \ln \Gamma(1-\lambda_2)}{\partial \lambda_2}$$

Methods of solving for the Lagrangian multipliers given in refs. (42, 43) are used to obtain the following:

For the individual data

$$M = 1.2050$$
$$\overline{\ln D_j} = 0.0594$$
$$\lambda_o = -0.79912$$
$$\lambda_1 = 3.40249$$
$$\lambda_2 = -3.10000$$

For the mean data

$$M = 1.2058$$
$$\overline{\ln D_j} = -0.06149$$
$$\lambda_o = 1.14028$$
$$\lambda_1 = 1.77476$$
$$\lambda_2 = -1.14000$$

The probability distribution for these two cases given in eqs. (4-61) and (4-63) are shown in Tables 5 and 6 and in Figs. 17 and 18 .

4.3 Reliability: In order to complete the description of damage distribution, reliability consideration is essential. This can also be thought of as the probability of survival, which can be expressed as

$$P(\overline{D}_k \geq \overline{D}_i) = R(\overline{D}_k)$$

where R = reliability

$\overline{D}_k$ = contesting damage

therefore $R(\overline{D}_k)$ = 1 - area under the probability curve between 0 and $\overline{D}_i$

Thus for a discrete case, the area can be approximated by summing the frequencies between the limits, hence

$$\text{Reliability, } R(\bar{D}_k) = 1 - \sum_j P(\bar{D}_j) \qquad (4\text{-}64)$$

This has been computed for the two probability distributions discussed earlier, and the results are shown in tables 5 and 6. It can be seen that the truncated normal distribution, which does not give a good approximation of damage distribution (see Figs. 16 and 18), yield a less desirable reliability.

4.3.1 Evaluation of Reliability (individual data):

Range of Damage	Reliability, % Actual	Gamma dist.
$\geq 0.30 \simeq (M-0.75s)$	99	98
≥ 0.40	95	96
≥ 0.50	90	92
$\geq 0.60 \simeq (M-0.5s)$	86	86
≥ 0.70	79	80
≥ 0.80	69	73
$\geq 0.90 \simeq (M-0.25s)$	58	65
$\geq 1.00 \simeq (M-0.1s)$	47	58

4.3.2 Evaluation of Reliability (mean data):

Range of Damage	Reliability, % Actual	Gamma dist.
$\geq 0.30 \simeq (M-0.75s)$	92	92
≥ 0.40	88	87
≥ 0.50	84	81
$\geq 0.60 \simeq (M-0.5s)$	82	75
≥ 0.70	78	69
≥ 0.80	73	63
$\geq 0.90 \simeq (M-0.25s)$	66	57
$\geq 1.00 \simeq (M-0.1s)$	58	51

4.3.3 Comparison of Safe Life Using Miner's Rule Based on Test Data:

Jacoby (44)	All types of materials, tests and stress conditions. (401 specimens)	95% safe for $D \geq 0.3$ 63% " " $D \geq 1.0$
Ahrensdorf (47)	Steel, Titanium and Aluminum alloy in block tests. (348 specimens)	95% safe for $D \geq 0.2$ 56% " " $D \geq 1.0$
This Study	Steel and Aluminum alloy (see Sec. 3.1.1)	99% safe for $D \geq 0.3$ 47% " " $D \geq 1.0$
	Steel and Aluminum alloy (see Sec. 3.1.1)	92% safe for $D \geq 0.3$ 58% " " $D \geq 1.0$

4.3.4 Discussion: A noticeable trend based on the above (section 4.3.1 and 4.3.2) is that over 90% of all data yield $\Sigma^n/_N \geq 0.3$. This agrees with the findings by Jacoby (44) who gave the probability as 95%, Brooks (45) as 99% probability and Mains (46) thus use of 0.3 will give better confidence in the use of linear law than when the value of 1.0 is assumed. This can be expressed as

$$\frac{(\Sigma\, n/N)_{\text{Design}}}{(\Sigma\, n/N)_{\text{Miner}}} = 0.3$$

and can be directly applied to programme and random loadings i.e.

$$N_F = \frac{0.3}{\Sigma \frac{\alpha_i}{N_i}} \quad \text{(Programme loading)}$$

$$N_F = \frac{0.3}{N_R} \left(\frac{\sqrt{2}\,\sigma}{S_R}\right)^b \Gamma\left(\frac{b}{2} + 1\right) \quad \text{(Random loading)}$$

In most observed data the above equations yield safe predictions.

The application of $\Sigma\, n/N = 0.3$ to prestress type loading seem unreasonable however, since the sum of initial prestress can be greater than 0.3. Nonetheless if 0.3 is thought of as a reduction factor in this case for remaining life prediction i.e.

$$n = [0.3\, n]_{\text{Miner}}$$

safe predictions can be guaranteed in most cases. For example after two initial prestress, n_1 and n_2 remaining life n_3 can be expressed as

$$n_3 = 0.3 \times [n_3]_{\text{Miner}}$$

$$= 0.3\, N_3 \left[1 - \frac{n_1}{N_1} - \frac{n_2}{N_2}\right]$$

Prestress type loading is generally not used for design of engineering structures so this discrepancy is not of great consequence.

V. CONCLUSION

Evidences from test results used here and in other publications sited show Miner's rule insufficient in predicting fatigue life. The other theories, which in general, require more experimental data or calculations give no better estimates either. This, as mentioned earlier, is a justification in the use of Miner's theory in fatigue design. The trend of cycle ratio summation is erratic and does not seem to depend entirely on the material, test type or stress range.

The use of the constant amplitude S-N test information has been shown to be a vital part of all the fatigue prediction theories discussed in the text. Consequently, it can be stated that more accurate predictions will depend on the accuracy of the S-N diagram. This diagram is known to be characterized by a significant amount of scatter of which the dominant factor is the type of loading. To obtain a more accurate S-N diagram therefore, will be at the expense of time and money. In the absence of this, the Miner's theory is adequate for initial estimates for designs but modified by some "safety factor". A lower bound "safety factor" of 3 seems appropriate from the above analysis for all types of loadings. This of course can be decreased where a fairly accurate amount of knowledge on the load spectrum is available.

REFERENCES

1. Miner, Milton A., "Cumulative Damage in Fatigue", Journal of Applied Mechanics, Vol. 12, No. 3, pp. A-159, September 1945.

2. Miles, John W., "On Structural Fatigue Under Random Loading", Journal of the Aeronautical Sciences, Vol. 1, pp. 753, November 1954.

3. Henry, D.L., "A Theory of Fatigue-Damage Accumulation in Steel", ASME Transactions, Vol. 77, No. 6, pp. 913-918, August 1955.

4. Crichlow, W.J., et al. "An Engineering Evaluation of Methods for the Prediction of Fatigue Life in Airframe Structures", ASD-TR-61-434, March 1962.

5. Corten, H.T. and Dolan, T.J., "Cumulative Fatigue Damage", Proceedings of the International Conference on Fatigue of Metals, Vol. 1, pp. 235, Institute of Mechanical Engineers, 1956.

6. Manson, S.S., et al. "A Proposed New Relation for Cumulative Fatigue Damage in Bending", Proceedings ASTM Vol. 61, pp. 679, 1961.

7. Valluri, Sitaram, R., "A Unified Engineering Theory of High Stress Level Fatigue", Aerospace Engineering, Vol. 20, No. 10, pp. 18, October 1961.

8. Freudenthal, A.M. and Heller, R.A., "On Stress Interaction in Fatigue and a Cumulative Damage Rule", Journal of the Aerospace Sciences, Vo. 26, No. 7, pp. 431, July 1959.

9. Grover, H.J., "An Observation Concerning the Cycle Ratio in Cumulative Damage", Symposium on Fatigue of Aircraft Structures, ASTM STP No. 274, pp. 120, 1959.

10. Grover, H.J., et al., "Fatigue Strength of Aircraft Materials; Axial-Load Fatigue Tests on Unnotched Sheet Specimens of 24 ST3 and 75 ST6 Aluminum Alloys and of SAE 4130 Steel, NACA TN 2324, March 1951.

11. Bennett, J.A., "A Study of the Damaging Effect of Fatigue Stressing on X4130 Steel", Proceedings, ASTM Vol. 46, pp. 693, 1946.

12. Richart, F.E. and Newmark, N.M., "An Hypothesis for the Determination of Cumulative Damage in Fatigue", Proceedings, ASTM Vol. 48, pp. 767, 1948.

13. Kommers, J.B., "The Effects of Overstress in Fatigue on the Endurance Life of Steel", Proceedings, ASTM Vol. 45, pp. 532, 1945.

14. Schijves, J. and Jacobs, J.A., "Research on Cumulative Damage in Fatigue of Riveted Aluminum Alloy Joints", National Aeronautical Research Institute, Amsterdam, Report No. NLL M 1999, 1955.

15. Fralich, R.W., "Experimental Investigation of Effects of Random Loading on the Fatigue Life of Notched Cantilever Beam Specimens of SAE 4130 Normalized Steel, NASA TN D663, February 1961.

16. Saunders, S.C., "A Review of Miner's Rule and Subsequent Generalization for Calculating Expected Fatigue Life", BSLR MIS Report No. 45, December 1970.

17. Bennett, J.A., "Effects of Fatigue-Stressing Short of Failure of Some Typical Aircraft Metals, NACA TN 992, October 1945.

18. Erickson, W.H., et al., "A Study of the Accumulation of Fatigue Damage in Steel", Proceedings, ASTM Vol. 61, pp. 704, 1961.

19. Liu, H.W. and Corten, H.T., "Fatigue Damage Under Varying Stress Amplitudes, NASA TN D647, November 1960.

20. Swanson, S.R., "An Investigation of the Fatigue of Aluminum Alloy due to Random Loading", UTIA Report No. 84, February 1963.

21. Swanson, S.R., "Systematic Axial Load Fatigue Tests Using Unnotched Aluminum Alloy 2024-T4 Extruded Bar Specimens, UTIA TN 35, May 1960.

22. Freudenthal, A.M., "Fatigue of Structural Metals Under Random Loading", Symposium on Acoustical Fatigue, ASTM STP 284, June 1960.

23. Crandall, S.H. and Mark, W.D., "Random Vibration in Mechanical Systems", Academic Press, Inc., 1963.

24. Bendat, J.S., "Probability Functions for Random Responses: Prediction of Peaks, Fatigue Damage, and Catastrophic Failures, NASA CR 33, April 1964.

25. Head, A.K. and Hooke, F.H., "Random Noise Fatigue Testing", Proceedings International Conference on Fatigue of Metals, pp. 301, 1956.

26. March, K.T., et al., "Exploratory Tests on the Effects of Random Loading and Corrosive Environment on Fatigue Strength of Fillet-Welded Lap Joints", Journal of Mechanical Engineering Science, Vol. 17, No. 4, pp. 881, August 1975.

27. White, D.J., and Lewszuk, J., "Cumulative Damage in Push-Pull Fatigue of Fillet-Welded Mild Steel Plate Subjected to Narrow Band Random Loading", Proceedings, Institute of Mechanical Engineers, Vol. 185, pp. 339, 1970-1971.

28. Kowalewski, J., "On The Relation between Fatigue Lives under Random Loading and Under Corresponding Program Loading", Proceedings of the Symposium on Full-Scale Fatigue Testing of Aircraft Structures, (F.J. Plantema and J. Schijve ed.), Pergamon Press, Ltd., 1961.

29. Hillberry, B.M., "Fatigue Life of 2024-T3, "Alloy Under Narrow and Broad Bond Random Loading", Symposium on Effects of Environmental and Complex Load History on Fatigue Life, ASTM STP 462, 1970.

30. Hardrath, H.F., et al., "Axial-Load Fatigue Tests of 2024-T3 and 7075-T6 Aluminum Alloy Sheet Specimens under Constant and Variable Stress Loads", NASA TN D-212, December 1959.

31. Liu, H.W., and Corten, H.T., "Fatigue Damage During Complex Stress Histories", NASA TN D-256, November 1959.

32. Rey, William K., "Cumulative Damage at Elevated Temperature", NACA TN 4284, September 1958.

33. Dolan, T.J., et al., "The Influence of Fluctuations in Stress Amplitude on the Fatigue of Metals", Proceedings, ASTM Vol. 49, pp. 646, 1949.

34. Schijves, J., and Jacobs, J.A., "Program-Fatigue Tests on Notched Light Alloy Specimens of 2024 and 7075 Material", National Aeronautical Research Institute, Amsterdam TR M2070 1960.

35. Dowling, N.E., "Fatigue Failure Predictions for Complicated Stress-Strain Histories", AD 736583, 1971.

36. Naumann, E.C., "Evaluation of the Influence of Load Randomization and of GAG Cycles on Fatigue Life", NASA TN D 1584, October 1964.

37. Freudenthal, A.M., and Heller, R.A., "On Stress Interaction in Fatigue and a Cumulative Damage Rule", WADC TR 58-69, pt. 1, (AD 155687), June 1958.

38. Freudenthal, A.M., and Heller, R.A., "On Stress Interaction in Fatigue and a Cumulative Damage Rule", WADC TR 58-69, pt. 2, June 1958.

39. Freudenthal, A.M., "A Random Fatigue Testing Procedure and Machine", Proceedings, ASTM Vol. 53, pp. 89, 1953.

40. Sherman, A.C., and Steiner, R., "Fatigue Life Under Random Loading for Several Power Spectral Shapes", NASA TR R-266, 1967.

41. Jaynes, E.T., "Probability Theory in Science and Engineering", McGraw-Hill Book Company, 1961.

42. Tribus, Myron, "Rational Descriptions, Decisions and Designs", Pergamon Press, Inc., 1969.

43. Tribus, Myron, et al., "The Use of Entropy in Hypothesis Testing", Proceedings of the National Symposium on Reliability and Quality Control in Electronics, Vol. 10, pp. 579, 1964.

44. Jacoby, G., "Comparison of Fatigue Life Estimation Processes for Irregularly Varying Loads", Proceedings of the Third Conference on Dimensioning and Strength Calculations, pp. 81, November 1968.

45. Brooks, P.D., "Structural Fatigue Research and Its Relation to Design", Proceedings of the International Conference on Fatigue in Aircraft Structure, (A.M. Freudenthal ed.), Academic Press, 1956.

46. Mains, R.M., "Mechanical Design for Random Loading", Random Vibrations (S.H. Crandall ed.), Technology Press of the Massachusetts Institute of Technology, 1958.

47. Ahrensdorf, K., "Fatigue Design Practice", Specialists Meeting on Design Against Fatigue, NATO AGARD-CP-141, December 1975.

$$S_i = -S_{i,min}$$

Table 3:

S(ksi)	N(cycles)
50	18770
45	33950
40	56030
35	114400
30	264800
25	671600
20	2711000

Valluri

$$S_{E,1} = S_{E,2} = 20 \text{ ksi}$$

$$S_i = S_{i,min}$$

Corten-Dolan

$$\delta = 5.8$$

Miner

$$b = 5.4$$

Table 4:

Miner

$$b = 5.54$$

hence $$N_F = \left(\frac{264}{\sqrt{2}\sigma}\right)^{5.54} \cdot \frac{1}{\Gamma(3.77)} = 5.75 \times 10^{12} \left(\frac{1}{\sqrt{2}\sigma}\right)^{5.54}$$

(see eq. 2-15)

Freudenthal

$\delta = 4.0$ (min. value, actual test value is 4.22)

$N_R = 1000$ cycles

$S_R = 51$ ksi (RMS)

To express S_R in eq. (2-52b) in terms of peak stress it has to be multiplied by $\sqrt{2}$

thus

$$N_F' = 1.79 \times 10^{10} \left(\frac{1}{\sqrt{2}\sigma}\right)^4$$

Corten-Dolan

$\delta = 5.67$

$N_R = 1000$ cycles

$S_R = 51$ ksi (RMS)

therefore

eq. (2-34) becomes

$$N_F' = 9.75 \times 10^{12} \left(\frac{1}{\sqrt{2}\sigma}\right)^{5.67}$$

It should be noted that the life predictions for random loading expressed above are in terms of ν_o^*, number of zero crossings with positive slope.